*Desalination and Water Treatment*
www.deswater.com

doi: 10.5004/dwt.2021.27764

238 (2021) 174–197
October

# High efficiency of the bioremoval process of Cu(II) ions with blackberry (*Rubus* L.) residues generated in the food industry

Tomasz Kalak

*Department of Industrial Products and Packaging Quality, Institute of Quality Science, Poznań University of Economics and Business, Niepodległości 10, 61-875 Poznań, Poland, email: tomasz.kalak@ue.poznan.pl*

Received 18 March 2021; Accepted 4 September 2021

**ABSTRACT**

In this research, blackberry (*Rubus* L.) pomace obtained during processing in the food industry was used to analyze the possibility of removing Cu(II) ions in biosorption processes. The properties of the biomaterial have been determined using selected analytical methods, such as elemental composition and mapping using scanning electron microscopy-energy dispersive X-ray spectroscopy, X-ray diffraction, surface area and pore volume analysis (Brunauer–Emmett–Teller, Barrett–Joyner–Halenda), thermogravimetry, electrokinetic zeta potential, scanning electron microscopy morphology and Fourier-transform infrared spectrophotometry. Several factors influencing the efficiency of the process were analyzed, such as biosorbent dosage, initial pH, initial metal concentration and contact time. As a result of the conducted research, the maximum biosorption efficiency was obtained at the level of 99.03%. The analysis of kinetics and the determined isotherms showed that the pseudo-second-order equation model and the Langmuir isotherm model best suited this process. To sum up, on the basis of the conducted experiments, blackberry biomass may be a suitable material for the effective removal of copper from wastewater and the improvement of water quality. This research is in line with current trends in the concepts of circular economy, sustainable development and climate neutrality.

*Keywords:* Water quality; Waste management; Cleaner environment; Biosorption efficiency; Blackberry residues; Cu(II) ions; Kinetics

## 1. Introduction

Globalization, dynamic development of industry and urbanization, as well as commercialization and consumerism, constantly cause serious environmental problems, such as discharge of municipal and industrial wastewater, which pollute aquatic environment [1]. Contamination of water reservoirs with heavy metals is one of the most dangerous environmental threats. Heavy metals threaten living organisms and human health and life due to their toxicity even in very low concentrations. They are highly toxic, non-biodegradable and released into the aquatic environment as a result of industrial activities are dangerous when they exceed permissible limits [2]. Copper is one of the most used metals in the world (next to iron and aluminum), and at the same time one of the most toxic elements, having a negative impact on the environment and human health [3]. Copper is essential for organisms to live, however its increased concentration levels damage cells and lead to Wilson's disease, hemolysis, hepatotoxic and nephrotoxic effects, extensive damage to the capillaries and the central nervous system as well as it causes many toxic and harmful effects by accumulating in brain, liver, pancreas and heart muscle [4,5]. Inhaling vapors containing Cu(II) ions may cause irritation, headache, dizziness, upset stomach, vomiting and diarrhea. In the case of oral

poisoning, there are symptoms of renal failure, and in the most severe cases, there is loss of consciousness and other disorders, even leading to loss of life [6]. The level of copper in the environment increases as a result of emissions from various industries, mining and production processes, fertilizer production and paper pulp as well as other human activities [7]. In waste and industrial wastewater, copper occurs mainly in the form of the divalent Cu(II) metal, which appears to be the most toxic. The ionic form is soluble in water and can be absorbed by living organisms. Due to the presence of Cu(II) toxicity, the United States Environmental Protection Agency (USEPA) has recommended a threshold concentration limit, defined as the maximum level of contamination at the level of 1.3 mg/L [8].

Treatment of metal-contaminated wastewater is usually done by various advanced and expensive technologies, such as solvent extraction, chemical precipitation, oxidation–reduction, electrodialysis, reverse osmosis, membrane techniques and ion exchange. Due to the high cost of these techniques, the search for cheaper and economical technologies is constantly being carried out. Undoubtedly, the biosorption process is one of them due to its low cost, ease of operation, no requirements for expensive equipment and versatility. In these processes, the biomass of various origins is used as a biosorbent, the use of which to remove heavy metals from the aquatic environment has been of great interest in recent years and is considered an extremely important matter for the future of the natural environment. Agricultural and municipal waste, as well as plant biomass, are rich in fibers capable of binding metal ions due to the presence of various functional groups, such as carbonyl, hydroxyl, carboxyl or amine groups. Many mechanisms can take place during the biosorption process, including physical interaction, chemisorption, ion exchange or complexation of metal ions to the functional groups of a biosorbent [9–15].

Food processing waste, including blackberry residues, is a promising biosorbent. Blackberries are mostly eaten fresh, but also can be processed and sold as freeze-dried, bulk frozen, puree as well as a juice, drink, or concentrate. In the industry, blackberries are used in the production of marmalade, jams, ice cream, dietary supplements and other confectionery and diet products [16]. The interest in blackberry and its waste is high due to the content of useful ingredients, such as ellagitannins, anthocyanins, vitamins, iron as well as other phenolic compounds (lignans, procyanidins, flavan-3-ols) that contribute to its high antioxidant capacity in ability to absorb oxygen radicals [17].

Strik et al. [18] reported that in 2005 global area planted and production of blackberry was estimated at 20,035 ha and 1,546,439 tons, with the highest production in Europe (7,692 ha, 47,399 tons) and North America (7,159 ha, 651,713 tons). Current data from 2020 indicate that the largest exporters of blackberries in the world are Spain (23.7% share), Mexico (18.3%), the United States (16.2%), Morocco (11.4%), Portugal (10.8%), the Netherlands (9.2%), Germany (1.9%), Belgium (1.9%), France (1.9%), South Africa (0.8%), Poland (0.8%), Guatemala (0.6%), Italy (0.5%), Serbia (0.5%) and United Kingdom (0.3%) [19]. It is estimated that about 25%–30% of the total weight of processed fruit and vegetables is waste from the food industry [20]. These huge amounts of waste need to be recycled and one alternative could be the use in biosorption processes to remove metal ions from wastewater and improve water quality.

The aim of this research was to study the possibility of removal of Cu(II) ions from water by the use of blackberry (*Rubus* L.) residues obtained from the processing in the food industry in Poland. The following factors, such as initial concentration of Cu(II) ions, biosorbent dosage, contact time, initial and equilibrium pH of tested solutions will be examined in the experiments in terms of their influence on biosorption processes. In addition, the goal was also to characterize the blackberry material by examining physico-chemical properties using several research methods such as elemental composition and mapping using scanning electron microscopy-energy dispersive X-ray spectroscopy (SEM-EDX) analysis, X-ray diffraction (XRD), specific surface area and pore volume (Brunauer–Emmett–Teller, Barrett–Joyner–Halenda), thermogravimetry, electrokinetic zeta potential, scanning electron microscopy (SEM) morphology, Fourier-transform infrared spectroscopy (FTIR). Furthermore, the purpose was to study adsorption kinetics by analyzing pseudo-first-order and pseudo-second-order reaction models as well as to describe equilibrium isotherms by the use of the Langmuir and Freundlich isotherm models.

## 2. Experimental procedure

### 2.1. Materials and methods

#### 2.1.1. Blackberry preparation

Blackberry (*Rubus* L.) residues were produced during processing in the food industry in Poland and used in these research studies. The process of crumbling, sieving and separation of biomass into different fractions was applied. Next, it was dried at a temperature of 60°C and stored in an exsiccator. The experiments were performed in triplicate and distilled water was used.

#### 2.1.2. Blackberry residues characterization

In the experiments, blackberry biomass particles with a diameter less than 0.212 mm were used. In the beginning, chemical and physical properties of the tested material were analyzed using several methods, such as total phenolic content (TPC), total antioxidant capacity, high-performance liquid chromatography (HPLC), the elemental composition and mapping using SEM-EDX analysis, XRD, specific surface area and pore volume (Brunauer–Emmett–Teller, Barrett–Joyner–Halenda), thermogravimetry, electrokinetic zeta potential, SEM morphology, FTIR spectrometry. The characteristics of the research methods and apparatus have been attached to this article as supplementary material (SM Methods).

#### 2.1.3. Cu(II) adsorption process

Blackberry residues were tested for the possibility of the removal of copper(II) ions from aqueous solutions in batch experiments at room temperature ($T$ = 23°C ± 1°C). For this reason, Cu(II) ions with analytical purity (standard for AAS 1 g/L, Sigma-Aldrich (Germany)) were applied. The blackberry residues (sample weight

in the range of 2.5–100 g/L) and a volume of Cu(II) solution (concentration in the range of 2.5–100 mg/L) at specific pH (2–5) were shaken in conical flasks for 60 min at rotation speed 150 rpm. The pH of Cu(II) initial solutions was adjusted with 0.1 M HCl and NaOH. Subsequently, phase separation was performed by centrifugation at 4,000 rpm. In the next phase, after biosorption in solutions separated from biomass, the concentration of Cu(II) ions (mg/L) was analyzed using the atomic absorption spectrophotometer SpectrAA 800 (F-AAS, at a wavelength λ = 324.8 nm for copper, Varian, Palo Alto, USA). The measurements were performed in triplicate and average results were finally reported.

The bioremoval efficiency $R$ (%) and sorption capacity $q_e$ (mg/g) was determined based on Eqs. (1) and (2), respectively:

$$R = \left[\frac{C_0 - C_e}{C_0}\right] \times 100\% \tag{1}$$

$$q_e = \frac{\left(C_0 - C_e\right) \times V}{m} \tag{2}$$

where $C_0$ and $C_e$ (mg/L) are initial and equilibrium Cu(II) ion concentrations, respectively; $V$ (L) is the volume of solution and $m$ (g) is the mass of blackberry biomass.

Isotherms and kinetics were determined using pseudo-first-order and pseudo-second-order, Langmuir and Freundlich models according to Eqs. (3)–(6), respectively:

$$q_t = q_e\left(1 - e^{k_1 t}\right) \tag{3}$$

$$q_t = \frac{q_e^2 k_2 t}{1 + q_e k_2 t} \tag{4}$$

$$q_e = \frac{q_{\max} K_L C_e}{1 + K_L C_e} \tag{5}$$

$$q_e = K_F C_e^{\frac{1}{n}} \tag{6}$$

where $q_t$ (mg/g) is the amount of Cu(II) ions adsorbed at any time $t$ (min); $q_e$ (mg/g) is the maximum amount of Cu(II) ions adsorbed per mass of the biosorbent at equilibrium; $k_1$ ($min^{-1}$) is the rate constant of pseudo-first-order adsorption; $k_2$ [g/(mg min)] is the rate constant of pseudo-second-order adsorption; $q_{max}$ (mg/g) is the maximum adsorption capacity; $K_L$ is the Langmuir constant; $C_e$ (mg/L) is the equilibrium concentration after the adsorption process; $K_F$ is the Freundlich constant and $1/n$ is the intensity of adsorption.

## 3. Results and discussion

### 3.1. Characterization of the biosorbent

In these studies, the blackberry biomaterial has been characterized using several analytical methods. Firstly, TPC was determined using the Folin–Ciocalteu's reagent and the result was 18.87 ± 0.12 mg/g in the dry mass of blackberry. Next, the total antioxidant capacity was determined using the ferric reducing ability of the plasma method and was equal to 132.41 ± 0.17 μmol AA/g (where AA is L-ascorbic acid).

In the next studies, dried blackberry material was extracted and analyzed using the HPLC method by comparing the retention times with standard chemical compounds in order to identify phenolic substances. Based on the analysis, the following chemicals were identified in the samples salicylic acid, syringic acid, ellagic acid, gallic acid, 3,4-dihydroxybenzoic acid, chlorogenic acid, ferulic acid, and salicylic acid, meta-, para- and ortho-coumaric acid, gallocatechin, catechin, vanillic acid, resveratrol. Some of these substances can be involved in the binding of metal ions in adsorption processes. Their presence in the blackberry material has also been confirmed in the literature. Various properties and compositions of raw blackberry in a 100 g sample are presented in Tables 1 [21] and S2 according to the United States Department of Agriculture (USDA) and the literature, respectively. Additionally, other authors published research results on composition in the literature. Vaillant [24] reported that protein content in blackberry fruit is small (approximately 1/100 g) and these substances are mainly membrane proteins from enzymes and cell walls involved in the metabolism of sugars, amino and organic acids. In addition, oxygen-scavenging enzymes were detected in blackberry juice, such as ascorbate peroxidase, dehydroascorbate reductase, glutathione peroxidase, glutathione reductase, glutathione, guaiacol peroxidase, monodehydroascorbate reductase and superoxide dismutase [25]. The main organic acid is malic acid and only traces of citric acid were reported [26]. The main role of organic acids is that they can help to preserve the bioactive compounds in the fruit during transformation and storage processes [24]. The dietary fiber content depends mainly on the degree of maturity of the fruit and is around 3–5 g/100 g. Dietary fibers, such as parietal polysaccharides, are mostly found in seeds and receptacles. Cellulose (2.2/100 g), pectin (0.3%) and xylose-based polymers are the main components of cell walls [27]. The content of arabinose and galactose derivatives is low [24]. The main ellagitannins include sanguiin H6, lambertianin C and oligomeric forms as well as other compounds were also reported, such as vescalagin, castalagin, pedunculagin, and lambertinanin A, D [28]. All ellagitannins are hydrolyzable tannins formed by hexahydroxydiphenic acid (the main backbone of the compound) and gallic acid [29]. Anthocyanins are one of the most important compounds in blackberries and are mainly responsible for their color. As the fruit ripens, these pigments increase in concentration significantly. The main anthocyanins mainly include cyaniding, however other compounds were also reported such as malvidin, pelargonidin, peonidin and delphinidin. Anthocyanidin units are attached to sugar moieties (glucose or disaccharide), to which aromatic or aliphatic acids can also be attached [30]. The main flavonoids are quercetin and catechin with all their derivatives. Furthermore, myricetin, kaempferol [31] and proanthocyanidin dimers up to hexamers (mainly in seeds) [27,32] were also reported in trace amounts. Phenolic acids include mainly hydroxybenzoic and hydroxycinnamic acids, derivatives of gallic acids, ferulic acid, p-coumaric acid, ellagic acid [22,23,27]. They occur also in conjugated forms, such as esters and

Table 1
Various properties and composition of raw blackberry in a 100 g sample according to United States Department of Agriculture (USDA) [21]

| Blackberry ingredients or properties | Content in a 100 g sample of raw blackberry |
|---|---|
| Calories | 43–64 kcal |
| Water | 85.5–91.9 g |
| Proteins | 1.18–1.64 g |
| Lipids | 0.37–0.63 g |
| Carbohydrates | 9.61 g |
| Fibers | 2.3–6.7 g |
| Sugars (Total) | 3.04–6.35 g |
| Sucrose | 0–0.14 g |
| Glucose | 1.53–3.02 g |
| Fructose | 1.51–3.05 g |
| Maltose | 0–0.14 g |
| Galactose | 0–0.11 g |
| Calcium (Ca) | 14–44 mg |
| Iron (Fe) | 0.33–0.78 mg |
| Magnesium (Mg) | 19–25 mg |
| Phosphorus (P) | 15–31 mg |
| Potassium (K) | 159–164 mg |
| Sodium (Na) | 1 mg |
| Zinc (Zn) | 0.42–0.64 mg |
| Copper (Cu) | 0.038–0.259 mg |
| Manganese (Mn) | 0.23–1.44 mg |
| Selenium (Se) | 0.1–0.7 μg |
| Vitamin C | 21 mg |
| Thiamin | 0.015–0.028 mg |
| Riboflavin | 0.02–0.036 mg |
| Niacin | 0.495–0.742 mg |
| Pantothenic acid | 0.217–0.347 mg |
| Vitamin B6 | 0.024–0.036 mg |
| Vitamin B9 (folic acid) | 11–34 mg |
| Folate (total) | 20–31 μg |
| Choline (total) | 8.5 mg |
| Betaine | 0.3 mg |
| Vitamin A | 3–17 μg |
| Carotene (beta) | 40–204 μg |
| Lutein + Zeaxanthin | 87–139 μg |
| Vitamin E | 0.56–1.83 mg |
| Tocopherol (total) | 1.51–2.67 mg |
| Vitamin K | 14.7–25.1 μg |
| Fatty acids (total saturated) | 0.014 g |

glycosides. Conjugated forms of hydroxycinnamic acids in lesser amounts (sinapic, caftaric and caffeic acids), as well as hydroxybenzoic acids (gentisic, syringic, salicylic, protocatechuic, vanillic, p-hydroxybenzoic acids), were also noted [27,31]. Secoisolariciresinol is recognized as the main lignan as well as matairesinol present in minor amounts [24,33]. Lipophilic compounds are mainly included in blackberry seeds (approx. 10% of the fresh fruit weight). 14%–15% oil is contained in blackberry seeds, in which a general content of lipids is equal to approx. 500 mg/100 g [24]. The enormous diversity in the chemical structures of blackberry biomass components (the presence of cellulose, lipids, proteins, carbohydrates, simple sugars, etc.) creates conditions that favor the binding of metal ions with the use of many functional groups, including phenolic, carboxyl, hydroxyl and others.

Elemental composition was determined using the SEM-EDX method (Fig. 1). The peaks present in the spectrum correspond to the elements, such as C, O, Mg, Al, Si, P, S, K, Ca, Fe and Cu, the composition of which was determined and shown in Table 2. As it is seen, the largest amounts are the elements carbon and oxygen, which is characteristic of organic matter. The determination of the content of elements was possible thanks to the number of counts in the energy-dispersive X-ray spectroscopy (EDX) microanalysis. Due to the fact that blackberry biomass is not a homogeneous material, slight quantitative differences in the composition may occur at each measuring point on the material surface. In addition, the SEM-EDX mapping method using a backscattered detector was used to determine the distribution of various elements on the material. Based on the analysis, different distribution of the particular elements (C, O, Mg, Al, Si, P, S, K, Ca, Fe, Cu) was observed. The intensity of the distribution varies and depends on the type of element and material properties (Fig. S1). It should be mentioned that the presence of copper in the examined blackberry residues is already useful information that this biomass is capable of binding Cu(II) ions.

X-ray diffraction analysis was performed and the diffractogram of the mineralogical composition of the biomass is attached as supplementary material of these studies (Fig. S2). In this analysis, in accordance with the intensity of reflexes, the approximate content of the individual phases was determined and presented. The basic phases of blackberry pomace are the following: quartz ($SiO_2$, 49.08%), whewellite ($CaC_2O_4 \cdot H_2O$, 31.46%), whewellite (syn. $CaC_2O_4 \cdot H_2O$, 19.46%).

The Brunauer–Emmett–Teller (BET) analysis was carried out and such isotherms as the low-temperature BET adsorption and desorption isotherm, the pore volume distribution (Barrett–Joyner–Halenda method) for adsorption and desorption as well as adsorption cumulative pore area, desorption cumulative pore volume (the Barrett–Joyner–Halenda method) were determined (Figs. S3–S9). The parameters obtained, such as specific surface area ($S_{BET}$), the volume of the pores ($V_p$) and average pore diameter ($A_{pd}$), are presented in Table 3. Adsorption and desorption isotherms correspond to type II adsorption behavior. Its intermediate flat portion of the curve relates to the formation of a monolayer. Pores with a diameter ranging from 2.0 to 50 nm were identified in the biomass, which means that they have been classified as mesopores [34].

Thermogravimetric analysis was carried out at a temperature ranging from 29°C to 600°C (Fig. S10). As a result of these measurements, a gradual loss of weight of the biomass material with increasing temperature was observed. The first phase of decomposition of the blackberry pomace occurred in the temperature range from 30°C to 120°C, and the second in the range of about 180°C–500°C, as shown

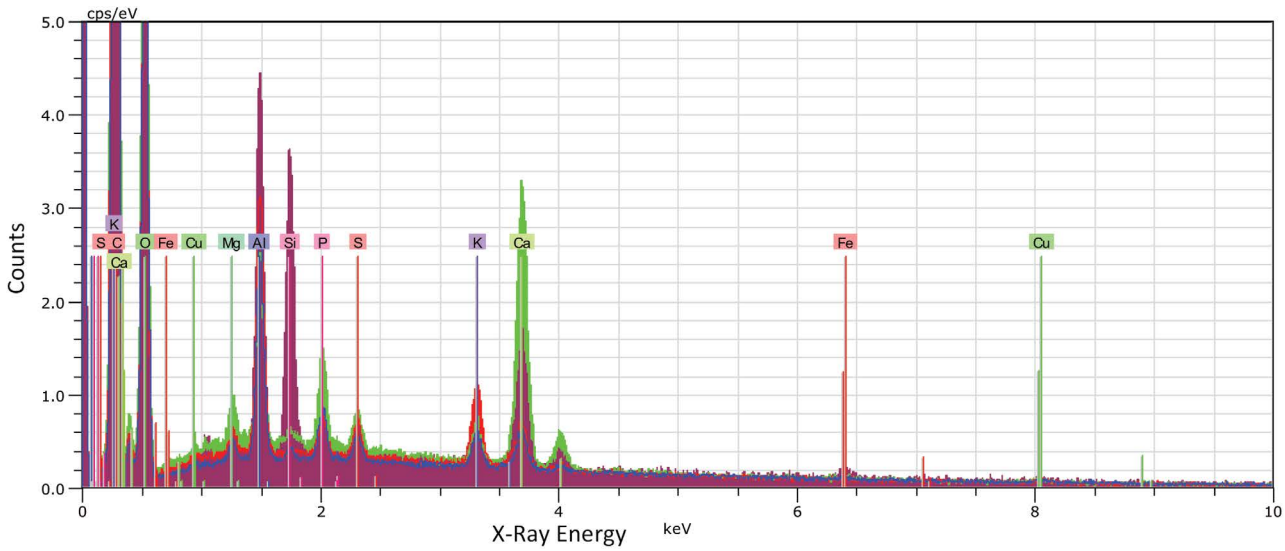


Fig. 1. SEM-EDX spectrum of blackberry residues.

Table 2
Average elemental composition of blackberry (determined by EDX microanalyzer)

| Elements | Content, weight (%) | Content, atomic (%) |
|---|---|---|
| C | 44.13 ± 1.73 | 52.71 ± 1.68 |
| O | 49.55 ± 1.47 | 44.48 ± 1.49 |
| Mg | 0.31 ± 0.09 | 0.18 ± 0.05 |
| Al | 2.06 ± 0.35 | 0.10 ± 0.191 |
| Si | 0.52 ± 0.07 | 0.27 ± 0.05 |
| P | 0.38 ± 0.07 | 0.18 ± 0.03 |
| S | 0.22 ± 0.01 | 0.10 ± 0.01 |
| K | 0.62 ± 0.14 | 0.23 ± 0.05 |
| Ca | 1.78 ± 0.08 | 0.64 ± 0.09 |
| Fe | 0.36 ± 0.09 | 0.09 ± 0.01 |
| Cu | 0.34 ± 0.040 | 0.08 ± 0.01 |

by the thermogravimetric analysis and differential thermal gravimetric (DTG) analysis curves. In the first stage, there was a slight decrease in weight equal to approx. 1.73%, which may result from evaporation of adsorbed water from the pomace sample. In the next phase, greater weight loss (approx. 37.88%) was observed, which was a consequence of the pyrolysis process ($CO_2$ release) and the evaporation of volatile substances. Jacques et al. [35] reported that in their studies the following volatile compounds were identified in blackberry: methyl ethyl ketone, heptane, toluene, hexanal, 2-hexenal, heptanal, 2-heptanone, 2-heptanol, methyl hexanoate, α-thujene, α-pinene, camphene, heptenal, benzaldehyde, 1-heptanol, β-myrcene, ethyl hexanoate, octanal, α-phellandrene, terpinolene, limonene, α-terpinene, 1-octanol, linalool oxide, ocimene, linalool, nonanal, trans-limonene oxide, isopinocarveol, nonenal, isoborneol, ethyl benzoate, terpinen-4-ol, p-cymen-8-ol, α-terpineol, methyl salicylate, decanal, verbenone, p-mentenal, (-)-carvone, geraniol, vitispirane, theaspirane, α-copaene and damascenone. Some or most of these substances may have evaporated within the temperature range of this process. At the temperature of 347°C, the thermogram shows a very intense peak (DTG) that relates to the breakdown of lipids, carbohydrates and proteins. Similar research results have been published in the literature [36,37].

The analysis of electrokinetic zeta potential (EZP) was carried out by combining electrophoresis and measuring the velocity of particles in liquid with a red laser (λ = 633 nm) based on the Doppler Effect (LDV). Determining this parameter is important for many industrial activities, including wastewater treatment in terms of environmental protection. EZP measurement is a useful method that can provide information about the interface of a material surface solution. This parameter can be used to predict and

Table 3
Adsorption and desorption parameters of blackberry residues

| Parameters | Values |
|---|---|
| BET specific surface area ($S_{BET}$) [$m^2/g$] | 0.1930 |
| Barrett–Joyner–Halenda adsorption volume of pores ($V_{pa}$) [$cm^3/g$] | 0.000152 |
| Barrett–Joyner–Halenda desorption volume of pores ($V_{pd}$) [$cm^3/g$] | 0.000208 |
| Barrett–Joyner–Halenda adsorption pore diameter ($A_{pa}$) [nm] | 10.266 |
| Barrett–Joyner–Halenda desorption pore diameter ($A_{pa}$) [nm] | 11.0427 |

control the stability of emulsions and suspensions, helping to understand the processes of aggregation and dispersion. This indicates the presence or absence of charged particles on the surface of materials and can therefore affect their performance and characteristics in suspension. The electrostatic charge value of EZP affects product specification, quality control and process control. This can ensure that relevant product performance and quality are maintained and improved. Furthermore, the importance of EZP for many applications has led to the development of various theories. Smoluchowski developed the theory on the relationship between EZP and electrophoretic mobility for very large rigid colloidal particles covered with a thin polymer layer [38]. On the other hand, Ohshima [39] proposed the soft particles theory, which determines the behavior of hard particles covered with an ion-permeable surface layer of polyelectrolytes. It makes it possible to determine the influence of surface charge on the metal ion sorption process and to determine its efficiency [40]. According to the literature, the aqueous slurry is more stable at higher zeta potential values, as electrostatically charged particles repel each other, overcoming the tendency to aggregate and agglomerate [41,42]. These studies showed that pH values had an influence on the surface charge, which gradually decreased from –3.18 mV (pH 2.05) to –30.3 mV (pH 6.92) (Fig. 2). The isoelectric point (IEP) is set at the zero points (no electrical charge) and represents the equilibrium balance between negative and positive ions (the system is the least stable). At the IEP point, the particles of the suspension are characterized by the lowest solubility, viscosity and osmotic pressure. In this analysis, the electrostatic charge did not reach the IEP and took only negative values below the IEP. This means that there is an advantage of positively charged particles over negatively charged ones on the biomass surface in the pH range from 2.0 to 7.0.

### 3.2. Biosorption studies of Cu(II) ions

#### 3.2.1. Effect of biosorbent dosage

Biosorbent dosage is an important parameter determining equilibrium between biosorbent and sorbate in the system, hence it is taken into account in sorption analysis. Therefore, the influence of blackberry dosage on biosorption efficiency of Cu(II) ions was investigated and Fig. 3 shows the results. The following conditions were used during the research: initial concentration of Cu(II) ions 10.0 mg/L, pH 2–5, agitation speed 150 rpm, $T$ = 23°C ± 1°C, contact time 60 min. In general, increasing blackberry dosage up to 40 g/L increased the biosorption efficiency. The results clearly show that the maximum sorption was reported at the dose of 40 g/L: 87.7% (pH 2), 92.5% (pH 3), 97.98% (pH 4), 95.4% (pH 5). Further increasing the dose of blackberry was not necessary as no further improvement was observed and optimization of the process was achieved. Besides, biosorption capacity decreased from 9.43 mg/g (dose 1 g/L, pH 4) to 0.22 mg/g (dose 40 g/L, pH 2) (Fig. 3b). The parameter was the highest at the smallest doses (1 g/L), while Cu(II) removal (%) was the lowest, which means that the saturation value was reached. This phenomenon can be attributed to the increased surface area of blackberry biosorbent, availability of more sorption sites as well as it may result from completed interactions of some factors. The decrease in biosorption capacity in the subsequent reactions can be attributed to aggregation or overlapping of active sites, resulting in a reduction in the total surface area of the biosorbent. At high sorbent dosages, the available amount of Cu(II) ions is insufficient to cover all

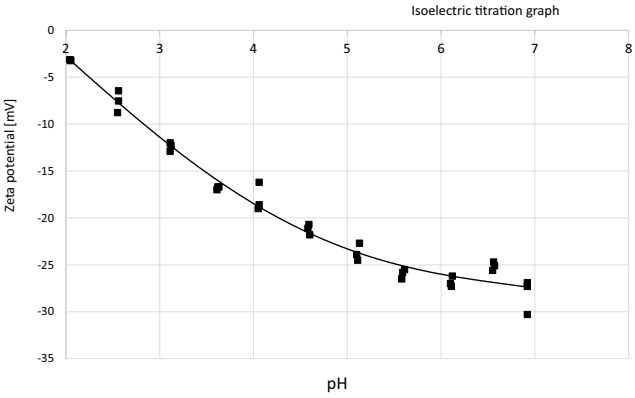


Fig. 2. The change in zeta potential with equilibrium pH.

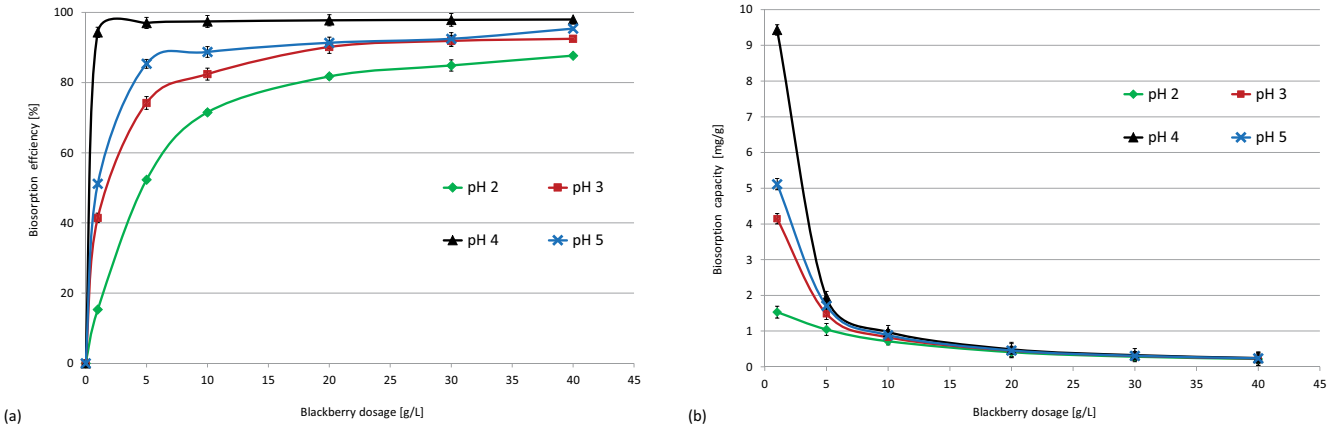


Fig. 3. The effect of blackberry dosage on biosorption efficiency (a) and biosorption capacity (b) of Cu(II) ions.

active sites on the biosorbent, which usually results in low absorption capacity. The results obtained in this way can be explained by the fact that biosorption capacity depends on both the concentration of adsorbed Cu(II) ions and biomass dosages. Analyzing all the results, the optimal value of biosorbent dosage can be estimated at 5 g/L at pH 4 (97%). In addition, under different pH and sorbent dosage conditions, the level of maximum sorption efficiency began to stabilize and was as follows: 40 g/L at pH 2 (87.7%) as well as 20 g/L at pH 3 (90.2%) and 5 (91.4%). These research results are similar to those published in the literature [6,37,43–47].

### 3.2.2. Effect of initial concentration of Cu(II)

Adsorption behavior under the different initial concentrations of Cu(II) ions was studied and the results are presented in Fig. 4. After analyzing the previous research results, it was decided to apply the following experimental conditions: initial concentration of Cu(II) ions (2.5–50 mg/L), adsorbent dosages 1–40 g/L, initial pH 4, contact time 60 min, rotation speed 150 rpm, $T = 23°C \pm 1°C$. An increase in adsorption efficiency was observed in the case of initial concentrations of 1 and 40 g/L. In other cases, there was no upward or downward trend, and the results remained stable (96.9%–98.24%). The equilibrium pH after all sorption processes ranged from 3.0 to 4.5. The highest removal equal to 99.03% was achieved for the biomass dosage of 40 g/L and initial concentrations of 25 and 50 g/L.

Based on this analysis of the biosorption process, it was found that the initial concentration of copper ions influences the saturation of the blackberry pomace surface. Probably the process of intramolecular diffusion of metal ions on the surface of the biomass takes place at higher concentrations. In a strongly acidic environment (pH 2), hydrolyzed ions may exist and diffuse much more slowly [48,49]. As shown in Fig. 4, the initial Cu(II) concentration was sufficient to initiate ion exchange at the interface between the aqueous and solid phases. Higher metal ion removal efficiency is proportional to the greater driving force of mass transfer and lower resistance to metal sorption [50]. Based on the literature, $Cu^{2+}$ ions have an ionic radius equal to 73 pm [51]. Many studies show that at the molecular level, the smaller the ionic radius of metal, the greater its propensity to hydrolyze in aqueous solutions. Hydrolyzed molecules have a lower ability to adsorption, which translates into a decrease in the efficiency of the biosorption process [51–53].

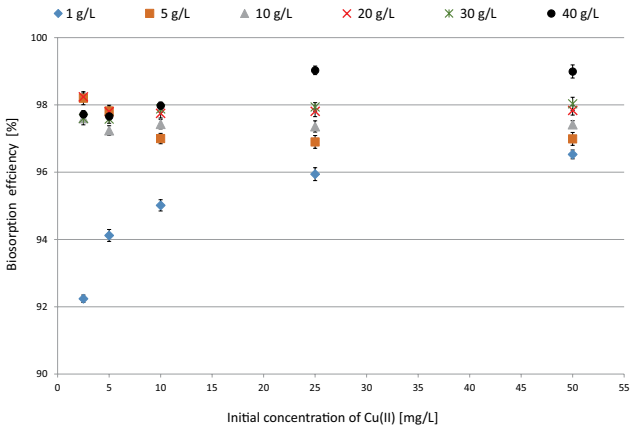


Fig. 4. The impact of initial concentration on the Cu(II) ions removal efficiency.

### 3.2.3. Analysis of pH profile

The pH parameter plays an important role in the biosorption process. Greater ionization of biomass functional groups occurs in solutions with lower pH, which favors biosorption. However, in alkaline solutions, Cu(II) metal has the ability to precipitate in the form of hydroxide [52]. Therefore, the influence of this factor on the efficiency of the process was investigated and the results are presented in Fig. 5. The applied conditions of the experiments were as follows: the initial concentration of Cu(II) ions 10.0 mg/L, blackberry dosage 1.0–40 g/L, pH range of 2–5, contact time 60 min, rotation speed 150 rpm, $T = 23°C \pm 1°C$. After analysis of the results, it was found that the best performance was obtained at pH 4.0 for the biosorbent doses of 1 g/L (94.3%), 5 g/L (97%), 10 g/L (97.4%), 20 g/L (97.7%), 30 g/L (97.9%) 40 g/L (97.98%). In all cases, an increase at pH 2 and 3, and a decrease in adsorption at pH 5 were demonstrated. At pH 2 the formation of copper chloride probably occurred which may make adsorption

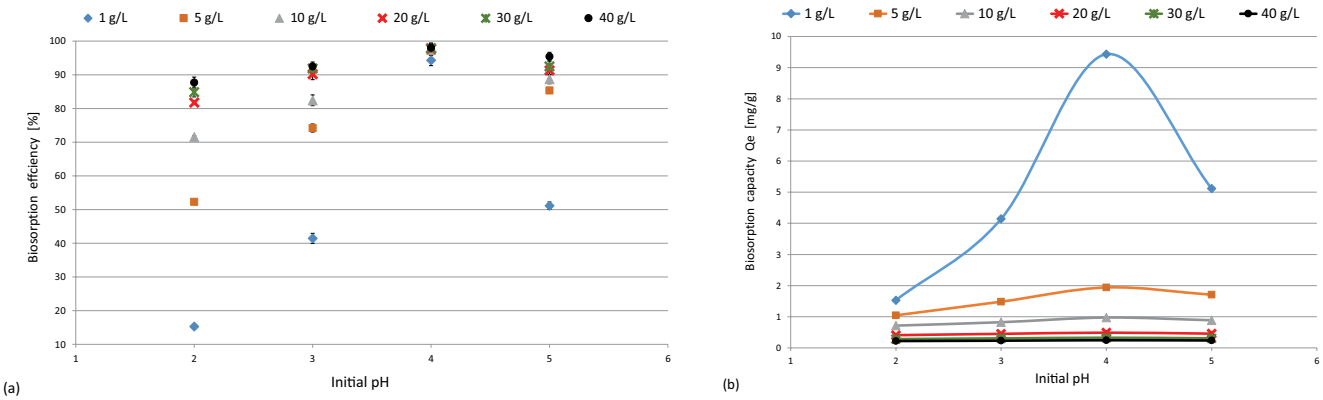


Fig. 5. The impact of initial pH on the Cu(II) removal efficiency (a) and biosorption capacity (b) at blackberry dosage 1.0–40 g/L.

more difficult. The adsorbent dosage of 1.0 g/L revealed the lowest efficiency. As it is seen in Fig. 5b, the highest biosorption capacity was observed at initial pH 4.0: 9.4 mg/g (1 g/L sorbent dosage), 1.94 mg/g (5 g/L), 0.97 mg/g (10 g/L), 0.49 mg/g (20 g/L), 0.33 mg/g (30 g/L), 0.24 mg/g (40 g/L). On the basis of the obtained results, the relationship between equilibrium pH and the highest biosorption efficiency obtained at initial pH 4.0 was investigated (Fig. 6). It was shown that at the initial concentration of Cu(II) 25–50 mg/L, equilibrium pH did not change in relation to the initial pH and remained at the level of pH 4.0. In the range of initial concentration of Cu(II) 2.5–20 mg/L, equilibrium pH increased to pH 4.1–4.5. On the other hand, in the range of initial concentration of Cu(II) 50–500 mg/L, equilibrium pH decreased to pH 3.0–3.9. Hence, the change in pH after the sorption processes in the examined systems was generally small. The highest adsorption efficiency was observed with a biosorbent dose of 40 g/L.

Most likely, the cation exchange mechanism was responsible for binding copper ions. The surface of the blackberry pomace and the functional groups were protonated by a significant amount of hydrogen ions, which resulted in an increase in the number of positively charged active centers and a decrease in the number of negatively charged centers. In an aqueous solution, Cu(II) ions compete with $H^+$ ions, which, due to electrostatic repulsion, do not favor the adsorption of positively charged copper ions. When the pH value was increased to 3–4, the surface became more negatively electrostatically charged, ion exchange took place and the acid groups were deprotonated, which made it possible to adsorb $Cu^{2+}$ ions in greater amounts. Based on the literature, in the pH range 2–5, copper exists in the ionic form, while at higher pH it precipitates as hydroxide. Hence, the maximum biosorption efficiency was obtained at pH 4. However, the decrease in sorption at pH 5 was probably due to the competition of hydroxyl ions at the active sites. The biosorption process can be hindered and slowed down by the presence of other forms of copper, such as $Cu(OH)^+$ and $Cu(OH)_2$. The mechanism of Cu(II) biosorption describing the influence of many factors (including pH) has been described in the literature [54–58].

### 3.2.4. Reaction kinetics

#### 3.2.4.1. Studies of contact time

The influence of contact time on biosorption was investigated, and the results are presented in Figs. 7 and S11. This parameter is important for the effective use of biosorbents in the industry. Determination of the optimal contact time in the process can be successfully used to determine the amount of solutions in adsorption processes, to design them, and also to effectively reduce the costs of the process [45,59,60]. Previous research has helped to establish the following optimal experimental conditions: initial concentration of Cu(II) 10 mg/L, initial pH 4.0, blackberry dosage 40 g/L, rotation speed 150 rpm, $T$ = 23°C ± 1°C. The obtained results confirmed the reports in the literature and the best adsorption efficiency was obtained for biomass with the smallest particle diameter less than 0.212 mm. The maximum sorption was obtained within the first 15 min of the process and there were no significant changes until 300 min. The results were as follows: <0.212 mm (98.7%), 0.212–0.3 mm (98.5%), 0.3–0.5 mm (97.9%). The equilibrium pH after adsorption ranged from 3.1 to 4.3. The rapid initial increase in adsorption could

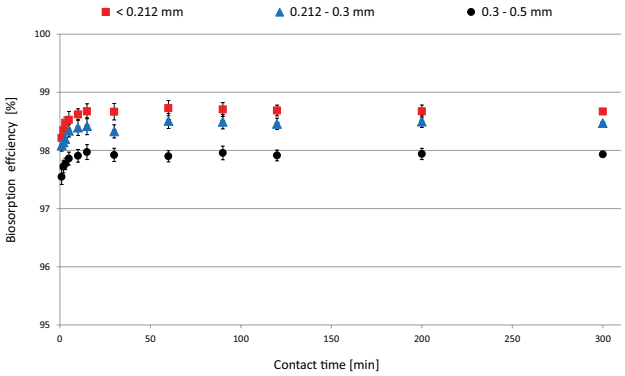


Fig. 7. The impact of contact time on the Cu(II) ions removal efficiency depending on the blackberry particle size.

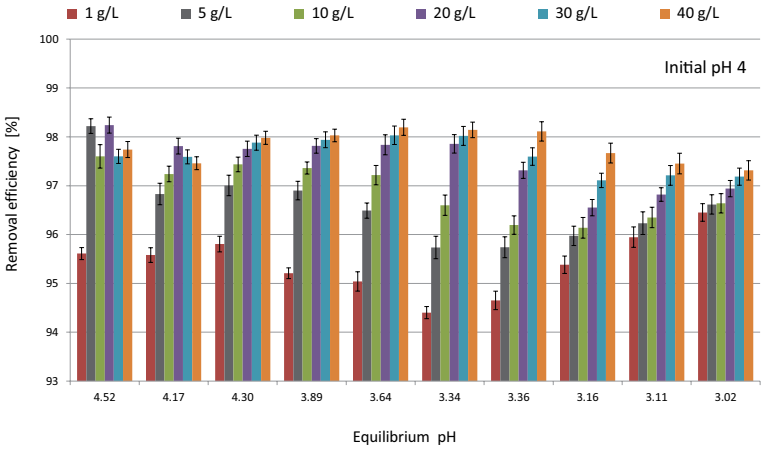


Fig. 6. The dependence between equilibrium pH and the Cu(II) removal efficiency (blackberry dosage 1.0–40 g/L; initial concentration of Cu(II) 2.5 mg/L (eq. pH 3.0–3.09)–500 mg/L (eq. pH 4.3–4.5)).

have been caused by the use of optimal process conditions, but also by the high concentration of copper ions at the interface and the availability of more free active sites on the surface of the biomass. The mechanism of the ion exchange reaction can take many forms, but the equilibrium of the process was achieved gradually by the occupation of active centers by cations [37,61].

*3.2.4.2. Pseudo-first-order and pseudo-second-order kinetic models*

Pseudo-first-order and pseudo-second-order models were used to analyze the kinetics of the sorption of Cu(II) ions on the blackberry. These mathematical models can describe the behavior of the biosorption process under various experimental conditions and are also very useful for process optimization. The results and kinetic parameters are shown in Figs. 8 & 9 and Table 4, respectively. In the first minutes of the process, biosorption was very fast and equilibrium was achieved after just 15 min for all ranges of tested particle sizes. The correlation coefficients for the pseudo-second-order kinetic model were relatively closest to 1.0, and the calculated $q_e$ values were also closer to the experimental $q$ values. These calculated values suggest that the sorption of Cu(II) ions is most consistent with the course of the pseudo-second-order reaction model. This model assumes that biosorption may be the rate-limiting step in the process. When investigating the effect of contact time on process efficiency, contact time, initial and equilibrium concentration of Cu(II) were experimental variables. $k_1$ values decreased with increasing blackberry particle size. Probably diffusion occurred during biosorption and this process was controlled by chemisorption. Cu(II) ions could have an affinity for active sites of the surface of blackberry pomace, which was associated with an increase in the coordination number with the surface. As a result, adhesion to the biosorbent surface took place and chemical bonds were formed [62,63].

*3.2.5. Isothermal studies*

Biosorption equilibrium of Cu(II) ions in relation to the blackberry biosorbent and the maximum sorption capacity was studied using Langmuir and Freundlich

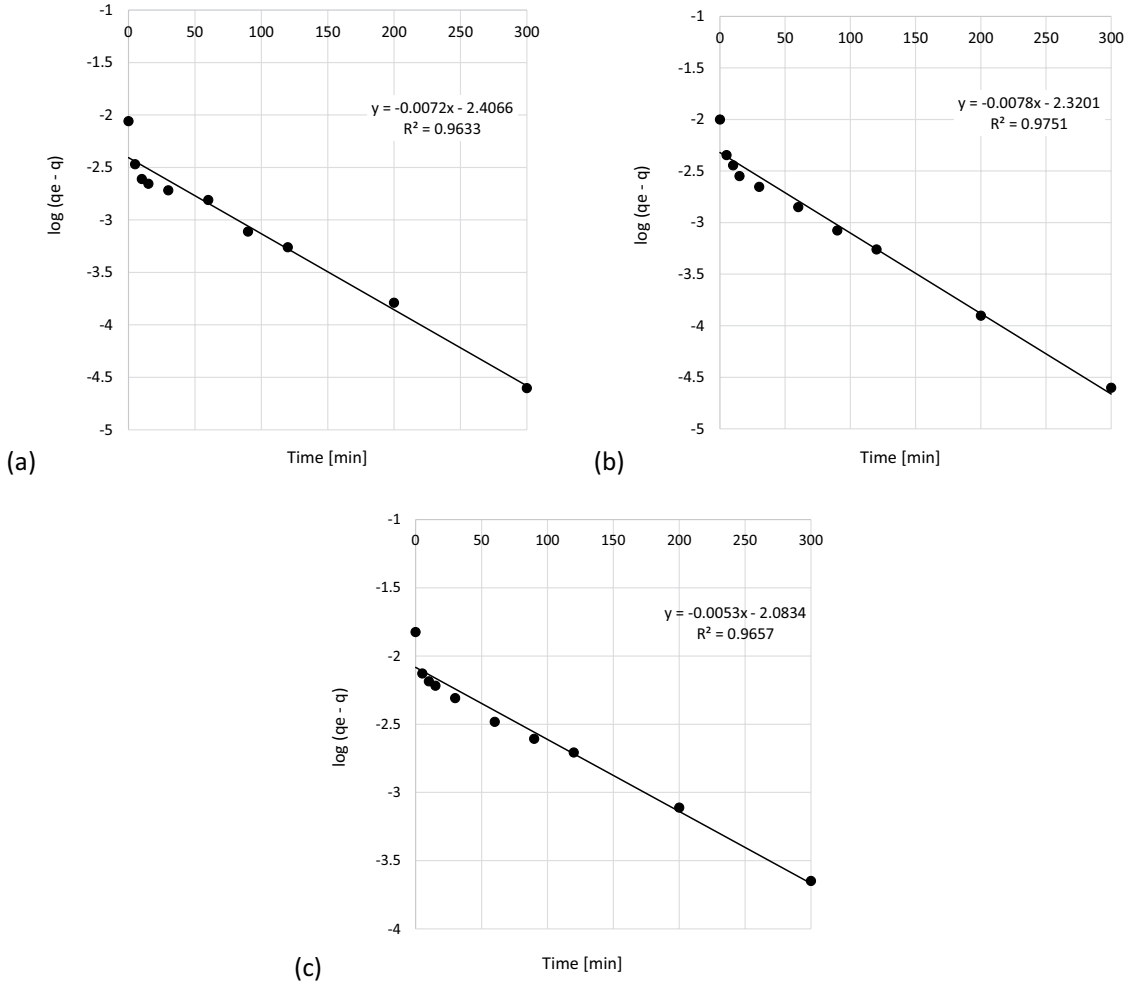


Fig. 8. Pseudo-first-order kinetic plot for the biosorption of Cu(II) with blackberry residues (biosorbent dosage 40 g/L; pH 4; initial concentration of Cu(II) 10 mg/L): (a) particle size range < 0.212 mm, (b) 0.212–0.3 mm, and (c) 0.3–0.5 mm.

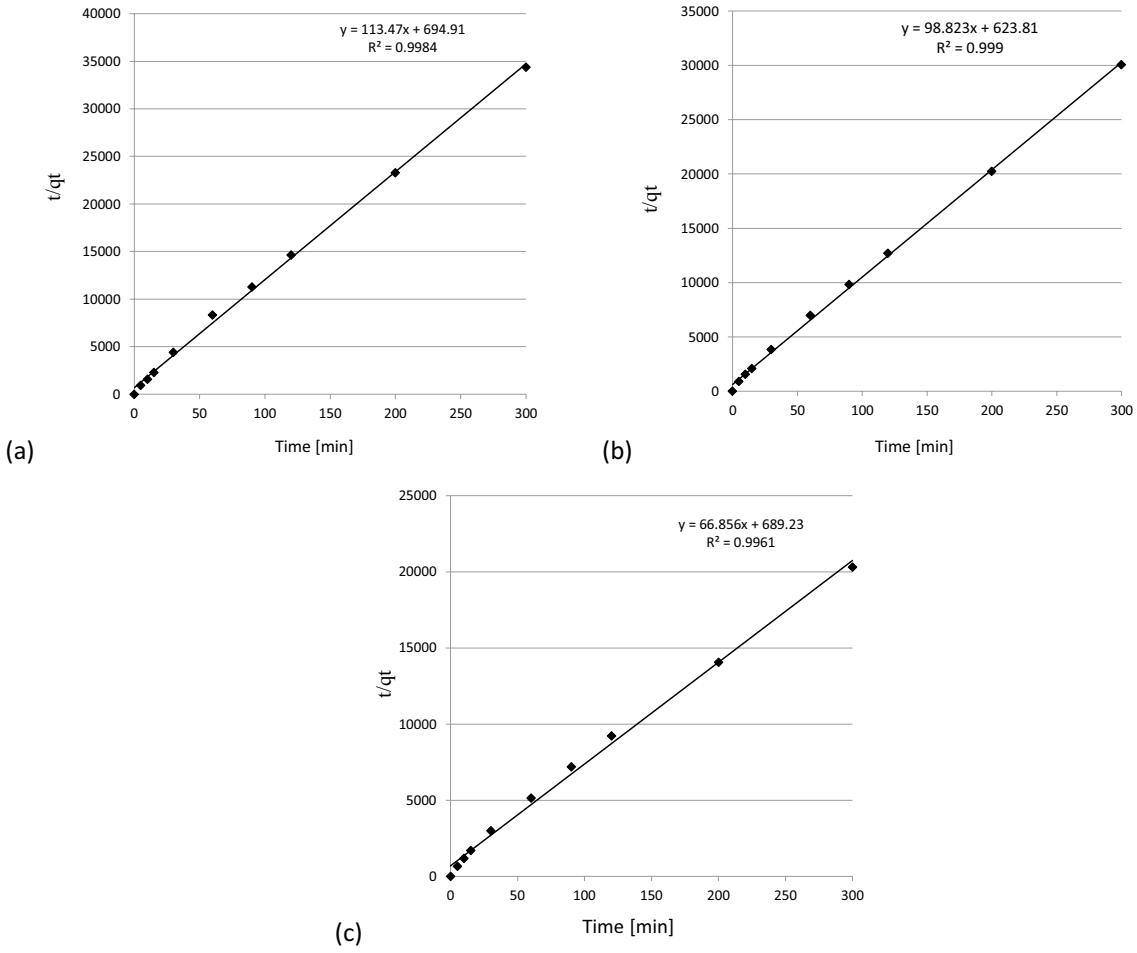


Fig. 9. Pseudo-second-order kinetic plot for the biosorption of Cu(II) with blackberry residues (biosorbent dosage 40 g/L; pH 4; initial concentration of Cu(II) 10 mg/L): (a) particle size range < 0.212 mm, (b) 0.212–0.3 mm, and (c) 0.3–0.5 mm.

isotherms models (Figs. S12–S19). Based on reported data, it was revealed that the Langmuir model is better suited to the biosorption process (Table 5). Other authors, such as Nadeem et al. [47], Ngah and Hanafiah [64], Salehi et al. [65] reported in their studies that biosorption equilibrium is also better described by the Langmuir model. One of the parameters of this model may be expressed by the constant ($R$) which is associated with the equilibrium parameter or dimension separation factor, where it is assumed that the biosorption system is favorable or unfavorable. The shape of the isotherm can be indicated by $R_L$ value as follows: unfavorable ($R_L > 1$), linear ($R_L = 1$), favorable ($0 < R_L < 1$), irreversible ($R_L = 0$). The data obtained in this research are in the range of $0 < R_L < 1$, which represents a favorable biosorption for the removal of Cu(II) ions [60,63]. According to the Langmuir equation, $K_L$ is the energy constant associated with the biosorption heat as well as the biosorbent and binding energy of the solute. The $K_L$ constant indicates the interaction between adsorbate and sorbent surfaces. A higher $K_L$ value indicates a strong interaction between them, while a lower value indicates weaker interaction [66]. On the other hand, the relationship between the concentration of dissolved ions on the surface of a biosorbent ($q_e$) and the concentration of metal ions dissolved in a liquid at equilibrium ($C_e$) is described by the Freundlich isotherm. Based on the calculated parameters ($n$ – sorption intensity index, $K_F$ – biomass sorption capacity index), it is suggested that the separation of Cu(II) ions from the reaction solution is undisturbed and quite easy. In these studies, the highest removal efficiency was equal to 96.7% (blackberry dosage 40 g/L, initial concentration 56 mg/L, initial pH 4) and 96.5% (40 g/L, 107 mg/L, pH 4). Table 6 compares the maximum Cu(II) adsorption capacity $q_{max}$ on blackberry with other selected results available in the literature. Clearly, the blackberry samples examined in this work have $q_{max}$ comparable to or higher than that of other biosorbents and commercial adsorbents.

### 3.3. SEM surface morphology

Blackberry pomace was analyzed using SEM morphology and images are shown in Fig. 10a–d. Generally speaking, biomass particles are characterized by irregular shapes of many sizes and a smooth surface. The structure is not homogeneous and developed flat surfaces are visible. Shape irregularities occur with smaller as well as larger

Table 4
Adsorption parameters of pseudo-first-order and the pseudo-second-order rate equations

| Particle size range (mm) | Adsorbent dosage (g/L) | Pseudo-first-order kinetic model | | | Pseudo-second-order kinetic model | | |
|---|---|---|---|---|---|---|---|
| | | $k_{ad}$ (min$^{-1}$) | $q_e$ (mg/g) | $R^2$ | $k$ (g/mg min) | $q_e$ (mg/g) | $R^2$ |
| <0.212 | 40 | 0.0166 | 0.0039 | 0.963 | 61,724.5 | 0.009 | 0.998 |
| 0.212–0.3 | 40 | 0.0180 | 0.0048 | 0.975 | 46,816.8 | 0.001 | 0.999 |
| 0.3–0.5 | 40 | 0.0122 | 0.0082 | 0.966 | 21,427.3 | 0.015 | 0.996 |

Table 5
Isotherm model constants and correlation coefficients for biosorption of Cu(II) using blackberry

| Adsorbent dosage (g/L) | Langmuir isotherm | | | Freundlich isotherm | | |
|---|---|---|---|---|---|---|
| | Calculated $q_m$ (mg/g) | $K_L$ (L/mg) | $R^2$ | $K_F$ (mg/g)(L/mg)$^{(1/n)}$ | $n$ | $R^2$ |
| 1 | 97.22 | 0.129 | 0.982 | 9.702 | 1.060 | 0.983 |
| 5 | 107.7 | 0.166 | 0.988 | 13.278 | 1.131 | 0.991 |
| 10 | 118.02 | 0.176 | 0.989 | 15.269 | 1.164 | 0.992 |
| 20 | 116.4 | 0.222 | 0.990 | 18.772 | 1.177 | 0.983 |

particles. The particles are joined into agglomerates of short, long, oval, polygonal lumps often resembling large, soft-edged crystals. Ferrari et al. [84] noticed similar observations of blackberry powder on SEM images.

### 3.4. FTIR analysis

The FTIR measurements of blackberry residues before and after the sorption process were carried out and Fig. 11 shows the spectra. The following experimental conditions were used to examine the samples: blackberry dose 40 g/L, initial concentration of Cu(II) ions 10 mg/L, initial pH 4, $T$ = 23°C ± 1°C, contact time 60 min. The description of the FTIR peaks is attached as supplementary material (Table S1). The spectra were analyzed before and after the biosorption process in terms of differences in shape, the intensity of bands, frequency and possible interaction of functional groups with Cu(II) ions. Fig. 11 shows that after the sorption process, the intensity of the bands shifted towards higher transmittance values, and their location remained at the same wavelengths or was slightly shifted. These changes can be identified as follows: 3,286.9 (shift to 3,286.05 cm$^{-1}$), 2,923.8 (shift to 2,923.3 cm$^{-1}$), 2,854.02 (shift to 2,853.4 cm$^{-1}$), 1,741.8 (shift to 1,742.5 cm$^{-1}$), 1,633.6 (shift to 1,641.8 cm$^{-1}$), 1,515.13 (shift to 1,514.48 cm$^{-1}$), 1,448.5 (shift to 1,452.24 cm$^{-1}$), 1,315.24 (shift to 1,316.35 cm$^{-1}$), 1,228.33 (shift to 1,225.95 cm$^{-1}$), 1,027.97 (shift to 1,032.99 cm$^{-1}$). The occurring phenomena of peak shifts can be explained by the interaction and bonding of Cu(II) ions with functional groups of compounds present in blackberry pomace, probably due to the process of chemisorption.

In the studied system, there was probably an ion-exchange mechanism between Cu(II) ions and cations (e.g., $Ca^{2+}$, $Mg^{2+}$), which is one of the essential mechanisms of Cu(II) sorption with blackberry residues. The presence of different cations was determined by the SEM-EDX method (Table 1). In addition, higher biosorption efficiency occurred at a lower initial pH 4.0 (Fig. 5), which indicated that ion exchange between protons or ionizable cations on the surface of blackberry biomass participates in Cu(II) sorption.

Blackberry particles contain a lot of negative charges on the surface (Fig. 2). Thus, it can be assumed that electrostatic attraction also could have occurred during the biosorption process. In this study, this biosorbent had the highest Cu(II) sorption capacity at initial pH 4.0, where

Table 6
Comparison of the Cu(II) ions adsorption capacity of different adsorbents

| Adsorbents | $q_{max}$ (mg/g) | Reference |
|---|---|---|
| Blackberry (*Rubus* L.) residues | 118.02 | These studies |
| Activated carbon from cassava peels | 8.0 | [67] |
| Barley straw | 4.6 | [68] |
| Carbonaceous nanocomposites | 146.1 | [69] |
| CMCD-MNPs | 47.2 | [70] |
| Graphene oxide | 74.9 | [71] |
| Graphene oxide aerogel | 19.7 | [72] |
| Modified activated carbon | 38 | [73] |
| $H_2SO_4$/$KMnO_4$-modified CNTs | 38.6 | [74] |
| Nanoporous activated neem bark | 21.23 | [75] |
| Olive stone | 0.0000319 | [76] |
| Orange peel | 4.64 | [77] |
| Pecan nutshell | 91.2 | [78] |
| Pomelo peel | 21.1 | [79] |
| Potato peel | 0.3877 | [80] |
| Rice husk | 13.003 | [81] |
| Rice shell (raw) | 17.42 | [82] |
| Sunflower hulls | 57.14 | [83] |

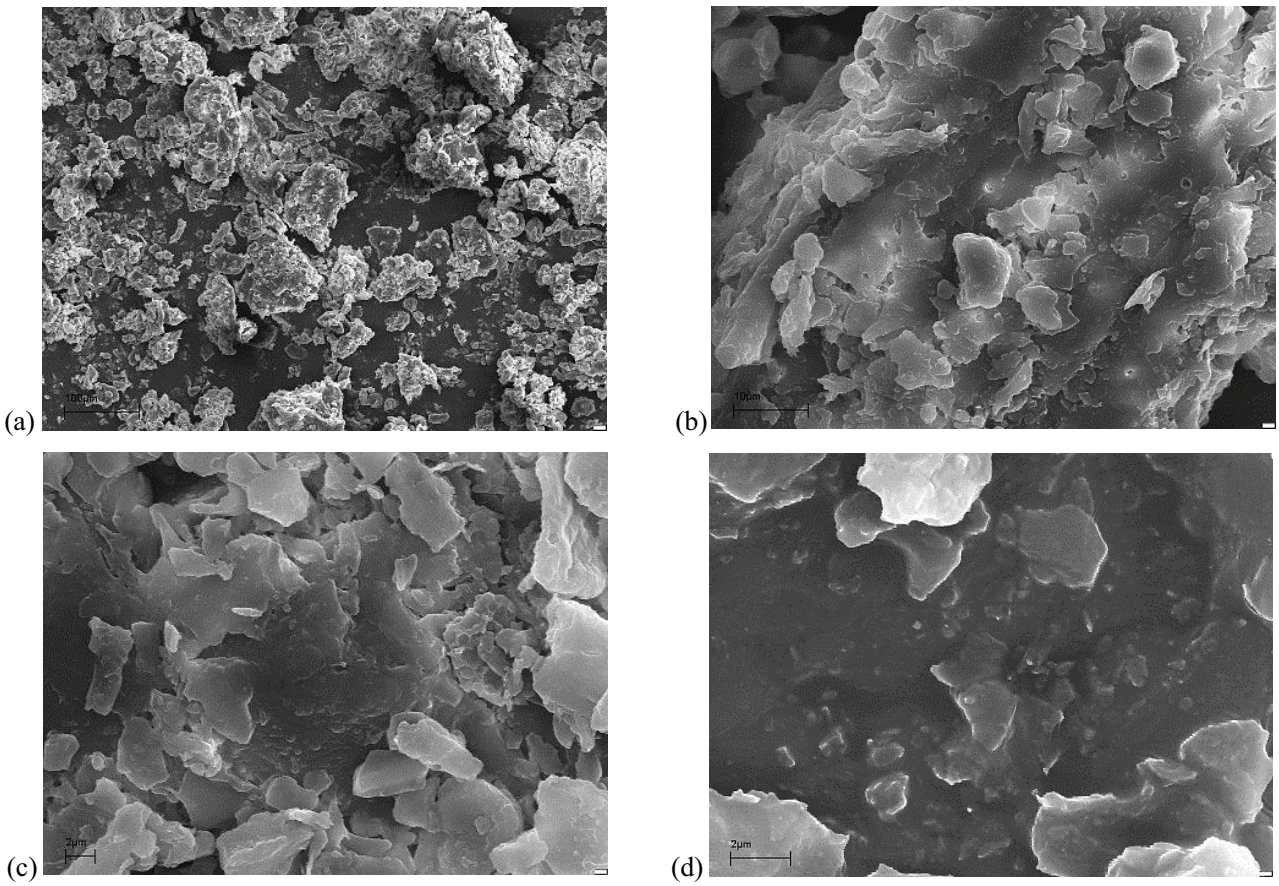


Fig. 10. SEM images of blackberry residues: (a) magn.: x500, scale bar: 100 μm, (b) x5000, 10 μm, (c) x10000, 2 μm, and (d) x20000, 2 μm.

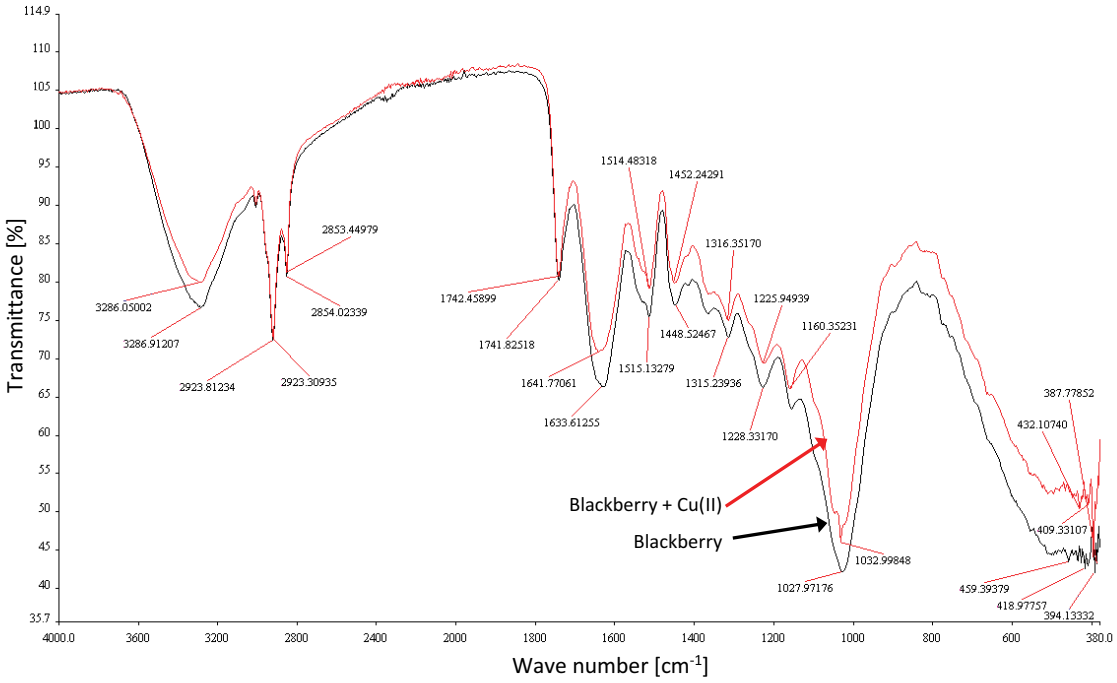


Fig. 11. FTIR spectrum of blackberry before and after Cu(II) ions adsorption.

the zeta potential in the range from –16 to –19 mV was recorded. This was probably due to the greater number of localized electrons, which could induce more Cu(II) ions sorbed on the blackberry surface [85].

Based on the results of these studies, the Cu(II) sorption mechanism can be described by probable ion-exchange Eqs. (7)–(9):

$$Cu^{2+} + BR_m - Ca \rightarrow BR_m - Cu + Ca^{2+} \quad (7)$$

$$Cu^{2+} + BR_m - Mg \rightarrow BR_m - Cu + Mg^{2+} \quad (8)$$

$$Cu^{2+} + BR_m - H + H_2O \rightarrow BR_m - Cu^{+} + H_3O^{+} \quad (9)$$

where: $BR_m$ corresponds to the blackberry residues matrix [86].

It is worth noting that the high sorption efficiency of Cu(II) ions is observed in various experimental conditions. Similar research results are reported in the literature [43,87,88]. This phenomenon is favored by the chemical properties of copper, which have a significant impact on its affinity to active sites. Furthermore, the electronegativity constant for Cu(II) is 1.90 which is responsible for electrostatic attraction [89]. As reported by other authors in the literature, chemisorption on the surface of blackberry pomace was probably the dominant mechanism in this study as well. Thus, the higher sorption capacity of Cu(II) is mainly influenced by other factors such as the first hydrolysis constant $pK_H$ 8.0 (negative logarithm of the hydrolysis constant) and the $Cu^{2+}$ ion radius (0.72 Å) [86,88,90]. These parameters make copper more easily adsorbed in biosorption reactions on the blackberry surface.

## 4. Conclusions

Blackberry (*Rubus* L.) waste obtained during processing in the food industry was taken into research for the analysis of the removal of Cu(II) ions from aqueous solutions. The physicochemical properties of the biosorbent were evaluated by the use of selected analytical methods. Such factors as biosorbent dosage, initial concentration of Cu(II) ions, initial pH and contact time were examined in terms of their influence on sorption processes. Based on the research results, it was observed that the maximum biosorption efficiency was 99.03% under the following conditions, such as initial pH 4.0, blackberry dosage 40 g/L, initial concentration range 25–50 mg/L, contact time 60 min, rotation speed 150 rpm, $T$ = 23°C ± 1°C. Generally speaking, the average process efficiency was above 90% under different experimental conditions. The possible sorption mechanism includes ion exchange, chemisorption and electrostatic attraction. The FTIR analysis showed changes in the intensity of bands and slight shifts of peaks, which can be a confirmation of Cu(II) ion binding. The kinetics analysis of the process revealed that the pseudo-second-order kinetic model and the Langmuir model fit the experimental data better. With the blackberry dose of 10 g/L, the maximum adsorption capacity $q_{max}$ = 118.02 mg/g (based on the Langmuir equation).

To conclude, it should be stated that the post-production blackberry waste is capable of removing Cu(II) ions with high process efficiency. The obtained research results create a real possibility of industrial use of blackberry waste to improve water quality, which is in line with the current global trends in sustainable development and circular economy.

## Acknowledgments

This research did not receive a specific grant from any funding agency in the public, commercial or not-for-profit sectors.

## Data availability statement

The data that support the findings of this study are available from the corresponding author upon reasonable request.

## References

[1] L. Centa Malucelli, L. Gustavo Lacerda, M. Dziedzic, M. Aurélio da Silva Carvalho Filho, Preparation, properties and future perspectives of nanocrystals from agro-industrial residues: a review of recent research, Rev. Environ. Sci. Biotechnol., 16 (2017) 131–145.
[2] T.K. Naiya, A.K. Bhattacharya, S.K. Das, Adsorption of Cd(II) and Pb(II) from aqueous solutions on activated alumina, J. Colloid Interface Sci., 333 (2009) 14–26.
[3] A. Mautner, H.A. Maples, H. Sehaqui, T. Zimmermann, U. Perez de Larraya, A.P. Mathew, C.Y. Lai, K. Li, A. Bismarck, Nitrate removal from water using a nanopaper ion-exchanger, Environ. Sci. Water Res. Technol., 2 (2016) 117–124.
[4] S. Larous, A.H. Meniai, M.B. Lehocine, Experimental study of the removal of copper from aqueous solutions by adsorption using sawdust, Desalination, 185 (2005) 483–490.
[5] F. Ekmekyapar, A. Aslan, Y.K. Bayhan, A. Cakici, Biosorption of copper(II) by nonliving lichen biomass of *Cladonia rangiformis hoffm*, J. Hazard. Mater., 137 (2006) 293–298.
[6] N. Benzidia, A. Salhi, S. Bakkas, L. Khamliche, Biosorption of copper Cu(II) in aqueous solution by chemically modified crushed marine algae (*Bifurcaria bifurcata*): equilibrium and kinetic studies, Mediterr. J. Chem., 4 (2015) 85–92.
[7] S. Pietrzyk, B. Tora, Trends in global copper mining – a review, IOP Conf. Ser.: Mater. Sci. Eng., 427 (2018) 012002.
[8] USEPA, EPA-822-R-01–001, Update of Ambient Water Quality Criteria for Copper, United States Environmental Protection Agency, April, 2001.
[9] G.R. de Freitas, M.G.C. da Silva, M.G.A. Vieira, Biosorption technology for removal of toxic metals: a review of commercial biosorbents and patents, Environ. Sci. Pollut. Res., 26 (2019) 19097–19118.
[10] M.S. Abdel-Raouf, A.R.M. Abdul-Raheim, Removal of heavy metals from industrial waste water by biomass-based materials: a review, J. Pollut. Eff. Control, 5 (2017) 1–13.
[11] A. Tripathi, M.R. Ranjan, Heavy metal removal from wastewater using low cost adsorbents, J. Biorem. Biodegrad., 6 (2015) 1–5.
[12] S. Ida, T. Eva, Removal of heavy metals during primary treatment of municipal wastewater and possibilities of enhanced removal: a review, Water, 13 (2021) 1121, doi: 10.3390/w13081121.
[13] N. Abdullah, N. Yusof, W.J. Lau, J. Jaafar, A.F. Ismail, Recent trends of heavy metal removal from water/wastewater by membrane technologies, J. Ind. Eng. Chem., 76 (2019) 17–38.
[14] M.A. Barakat, New trends in removing heavy metals from industrial wastewater, Arabian J. Chem., 4 (2011) 361–377.
[15] A.R. Lucaci, D. Bulgariu, M.-C. Popescu, L. Bulgariu, Adsorption of Cu(II) ions on adsorbent materials obtained

from marine red algae *Callithamnion corymbosum* sp., Water, 12 (2020) 372, doi: 10.3390/w12020372.
[16] E. Kafkas, M. Koşar, N. Türemiş, K.H.C. Başer, Analysis of sugars, organic acids and vitamin C contents of blackberry genotypes from Turkey, Food Chem., 97 (2006) 732–736.
[17] M.J. Cho, L.R. Howard, R.L. Prior, J.R. Clark, Flavonoid glycosides and antioxidant capacity of various blackberry and red grape genotypes determined by high-performance liquid chromatogrphy/mass spectrometry, J. Sci. Food Agric., 84 (2004) 1771–1782.
[18] B.C. Strik, J.R. Clark, C.E. Finn, M.P. Bañados, Worldwide Blackberry Production, HortTechnology, 17 (2007) 205–213.
[19] Blackberry, Overview of Global Blackberry Market. Available at: https://www.tridge.com/intelligences/blackberry (accessed: November 17, 2020).
[20] N.A. Sagar, S. Pareek, S. Sharma, E.M. Yahia, M.G. Lobo, Fruit and vegetable waste: bioactive compounds, their extraction, and possible utilization, Compr. Rev. Food Sci. Food Saf., 17 (2018) 512–531.
[21] USDA, National Nutrient Database, United States Department of Agriculture, 2021. Available at: http://fdc.nal.usda.gov (accessed June 10, 2021).
[22] C. Mertz, V. Cheynier, Z. Günata, P. Brat, Analysis of phenolic compounds in two blackberry species (*Rubus glaucus* and *Rubus adenotrichus*) by high-performance liquid chromatography with diode array detection and electrospray ion trap mass spectrometry, J. Agric. Food Chem., 55 (2007) 8616–8624.
[23] S. Sellappan, C.C. Akoh, G. Krewer, Phenolic compounds and antioxidant capacity of Georgia-grown blueberries and blackberries, J. Agric. Food Chem., 50 (2002) 2432–2438.
[24] F. Vaillant, Chapter 25 – Blackberries, A.K. Jaiswal, Ed., Nutritional Composition and Antioxidant Properties of Fruits and Vegetables, Academic Press, London, United Kingdom, 2020, pp. 407–422, doi: 10.1016/B978-0-12-812780-3.00025-8.
[25] H. Jiao, S.Y. Wang, Correlation of antioxidant capacities to oxygen radical scavenging enzyme activities in blackberry, J. Agric. Food Chem., 48 (2000) 5672–5676.
[26] M.A. Romero Rodriguez, M.L. Vazquez Oderiz, J. Lopez Hernandez, J. Simal Lozano, Determination of vitamin C and organic acids in various fruits by HPLC, J. Chromatogr. Sci., 30 (1992) 433–437.
[27] M. Zia-Ul-Haq, M. Riaz, V. De Feo, H.Z.E. Jaafar, M. Moga, *Rubus fruticosus* L.: constituents, biological activities and health related uses, Molecules, 19 (2014) 10998–11029.
[28] T.J. Hager, L.R. Howard, R. Liyanage, J.O. Lay, R.L. Prior, Ellagitannin composition of blackberry as determined by HPLC-ESI-MS and MALDI-TOF-MS, J. Agric. Food Chem., 56 (2008) 661–669.
[29] C. García-Muñoz, F. Vaillant, Metabolic fate of ellagitannins: implications for health, and research perspectives for innovative functional foods, Crit. Rev. Food Sci. Nutr., 54 (2014) 1584–1598.
[30] J. Lee, M. Dossett, C.E. Finn, *Rubus* fruit phenolic research: the good, the bad, and the confusing, Food Chem., 130 (2012) 785–796.
[31] L. Kaume, L.R. Howard, L. Devareddy, The blackberry fruit: a review on its composition and chemistry, metabolism and bioavailability, and health benefits, J. Agric. Food Chem., 60 (2012) 5716–5727.
[32] E.O. Cuevas-Rodríguez, G.G. Yousef, P.A. García-Saucedo, J. López-Medina, O. Paredes-López, M.A. Lila, Characterization of anthocyanins and proanthocyanidins in wild and domesticated Mexican blackberries (*Rubus* spp.), J. Agric. Food Chem., 58 (2010) 7458–7464.
[33] W.M. Mazur, M. Uehara, K. Wähälä, H. Adlercreutz, Phyto-oestrogen content of berries, and plasma concentrations and urinary excretion of enterolactone after a single strawberry-meal in human subjects, Br. J. Nutr., 83 (2000) 381–387.
[34] K.S.W. Sing, Reporting physisorption data for gas/solid systems with special reference to the determination of surface area and porosity, Pure Appl. Chem., 54 (1982) 2201–2218.
[35] A.C. Jacques, F.C. Chaves, R.C. Zambiazi, M.C. Brasil, E.B. Caramão, Bioactive and volatile organic compounds in Southern Brazilian blackberry (*Rubus fruticosus*) fruit cv. Tupy, Food Sci. Technol., 34 (2014) 636–643.
[36] F.M. Cui, X.Y. Zhang, L.M. Shang, Thermogravimetric analysis of biomass pyrolysis under different atmospheres, Appl. Mech. Mater., 448–453 (2013) 1616–1619.
[37] T. Kalak, J. Dudczak-Halabuda, Y. Tachibana, R. Cierpiszewski, Residual biomass of gooseberry (*Ribes uva-crispa* L.) for the bioremoval process of Fe(III) ions, Desal. Water Treat., 202 (2020) 345–354.
[38] I. Ostolska, M. Wiśniewska, Application of the zeta potential measurements to explanation of colloidal $Cr_2O_3$ stability mechanism in the presence of the ionic polyamino acids, Colloid Polym. Sci., 292 (2014) 2453–2464.
[39] H. Ohshima, Limiting electrophoretic mobility of a highly charged particle in an electrolyte solution: solidification effect, J. Colloid Interface Sci., 349 (2010) 641–644.
[40] M. Erdemoglu, M. Sarikaya, Effects of heavy metals and oxalate on the zeta potential of magnetite, J. Colloid Interface Sci., 300 (2006) 795–804.
[41] Ö. Demirbaş, M. Alkan, M. Doğan, Y. Turhan, H. Namli, P. Turan, Electrokinetic and adsorption properties of sepiolite modified by 3-aminopropyltriethoxysilane, J. Hazard. Mater., 149 (2007) 650–656.
[42] T. Kalak, A. Kłopotek, R. Cierpiszewski, Effective adsorption of lead ions using fly ash obtained in the novel circulating fluidized bed combustion technology, Microchem. J., 145 (2019) 1011–1025.
[43] A.A. Al-Homaidan, H.J. Al-Houri, A.A. Al-Hazzani, G. Elgaaly, N.M.S. Moubayed, Biosorption of copper ions from aqueous solutions by *Spirulina platensis* biomass, Arabian J. Chem., 7 (2014) 57–62.
[44] K. Naseem, R. Huma, A. Shahbaz, J. Jamal, M.Z. Ur Rehman, A. Sharif, E. Ahmed, R. Begum, A. Irfan, A. Al-Sehemi, Z.H. Farooqi,. Extraction of heavy metals from aqueous medium by husk biomass: adsorption isotherm, kinetic and thermodynamic study, Z. Phys. Chem., 233 (2018) 201–223.
[45] S. Aslan, S. Yildiz, M. Ozturk, Biosorption of $Cu^{2+}$ and $Ni^{2+}$ ions from aqueous solutions using waste dried activated sludge biomass, Pol. J. Chem. Technol., 20 (2018) 20–28.
[46] H.A. El-Araby, A.M. Ibrahim, A. Mangood, A. Abdel-Rahman, Sesame husk as adsorbent for copper(II) ions removal from aqueous solution, J. Geosci. Environ. Prot., 5 (2017) 109–152.
[47] R. Nadeem, M.A. Hanif, A. Mahmood, M.S. Jamil, M. Ashraf, Biosorption of Cu(II) ions from aqueous effluents by blackgram bran (BGB), J. Hazard. Mater., 168 (2009) 1622–1625.
[48] V. Mînzatu, C.-M. Davidescu, P. Negrea, M. Ciopec, C. Muntean, I. Hulka, C. Paul, A. Negrea, N. Duteanu, Synthesis, characterization and adsorptive performances of a composite material based on carbon and iron oxide particles, Int. J. Mol. Sci., 20 (2019) 1609–1621.
[49] N.S. Langeroodi, Z. Farhadravesh, A.D. Khalaji, Optimization of adsorption parameters for Fe(III) ions removal from aqueous solutions by transition metal oxide nanocomposite, Green Chem. Lett. Rev., 11 (2018) 404–413.
[50] T.C. Egbosiuba, A.S. Abdulkareem, A.S. Kovo, E.A. Afolabi, J.O. Tijani, M.T. Bankole, S. Bo, W.D. Roos, Adsorption of Cr(VI), Ni(II), Fe(II) and Cd(II) ions by KIAgNPs decorated MWCNTs in a batch and fixed bed process, Sci. Rep., 11 (2021) 2045–2322.
[51] K. Mathivanan, R. Rajaram, V. Balasubramanian, Biosorption of Cd(II) and Cu(II) ions using *Lysinibacillus fusiformis* KMNTT-10: equilibrium and kinetic studies, Desal. Water Treat., 57 (2016) 22429–22440.
[52] M. Salman, R. Rehman, U. Farooq, A. Tahir, L. Mitu, Biosorptive removal of cadmium(II) and copper(II) using microwave-assisted thiourea-modified *Sorghum bicolor* agrowaste, J. Chem., 2020 (2020) 8269643, doi: 10.1155/2020/8269643.
[53] T. Kalak, J. Dudczak-Hałabuda, Y. Tachibana, R. Cierpiszewski, Effective use of elderberry (*Sambucus nigra*) pomace in biosorption processes of Fe(III) ions, Chemosphere, 246 (2020) 125744, doi: 10.1016/j.chemosphere.2019.125744.
[54] L. Dong, Z. Diao, J. Du, Z. Jiang, Q. Meng, Y. Zhang, Mechanism of Cu(II) Biosorption by *Saccharomyces cerevisiae*,

3rd International Conference on Bioinformatics and Biomedical Engineering, IEEE, Beijing, China, 2009, pp. 1–4.
[55] C. Tu, Y. Liu, J. Wei, L. Li, K.G. Scheckel, Y. Luo, Characterization and mechanism of copper biosorption by a highly copper-resistant fungal strain isolated from copper-polluted acidic orchard soil, Environ. Sci. Pollut. Res. Int., 25 (2018) 24965–24974.
[56] J.B. Dulla, M.R. Tamana, S. Boddu, K. Pulipati, K. Srirama, Biosorption of copper(II) onto spent biomass of *Gelidiella acerosa* (brown marine algae): optimization and kinetic studies, Appl. Water Sci., 10 (2020) 56, doi: 10.1007/s13201-019-1125-3.
[57] M. Isam, L. Baloo, S.R.M. Kutty, S. Yavari, Optimisation and modelling of Pb(II) and Cu(II) biosorption onto red algae (*Gracilaria changii*) by using response surface methodology, Water, 11 (2019) 2325, doi: 10.3390/w11112325.
[58] X.H. Wang, R.H. Song, S.X. Teng, M.M. Gao, J.Y. Ni, F.F. Liu, S.G. Wang, B.Y. Gao, Characteristics and mechanisms of Cu(II) biosorption by disintegrated aerobic granules, J. Hazard. Mater., 179 (2010) 431–437.
[59] J.M. do Nascimento, J.D. de Oliveira, A.C.L. Rizzo, S.G.F. Leite, Biosorption Cu(II) by the yeast *Saccharomyces cerevisiae*, Biotechnol. Rep., 21 (2019) e00315, doi: 10.1016/j.btre.2019.e00315.
[60] O.A. Mohamad, X. Hao, P. Xie, S. Hatab, Y. Lin, G. Wei, Biosorption of copper(II) from aqueous solution using non-living *Mesorhizobium amorphae* strain CCNWGS0123, Microbes Environ., 3 (2012) 234–241.
[61] Z. Velkova, M. Stoytcheva, V. Gochev, Biosorption of Cu(II) onto chemically modified waste mycelium of *Aspergillus awamori*: equilibrium, kinetics and modeling studies, J. Biosci. Biotech., 1 (2012) 163–169.
[62] A. Dąbrowski, Adsorption – from theory to practice, Adv. Colloid Interface Sci., 93 (2001) 135–224.
[63] Y.S. Ho, J.C.Y. Ng, G. McKay, Kinetics of pollutant sorption by biosorbents: review, Sep. Purif. Rev., 29 (2000) 189–232.
[64] W.S.W. Ngah, M.A.K.M. Hanafiah, Surface modification of rubber (*Hevea brasiliensis*) leaves for the adsorption of copper ions: kinetic, thermodynamic and binding mechanisms, J. Chem. Technol. Biotechnol., 84 (2009) 192–201.
[65] P. Salehi, B. Asghari, F. Mohammadi, Removal of heavy metals from aqueous solutions by *Cercis siliquastrum* L., J. Iran. Chem. Soc., 5 (2008) 80–86.
[66] A.S.A. Aziz, L.A. Manaf, H.C. Man, N.S. Kumar, Kinetic modeling and isotherm studies for copper(II) adsorption onto palm oil boiler mill fly ash (POFA) as a natural low-cost adsorbent, BioResources, 9 (2013) 336–356.
[67] H.I. Owamah, Biosorptive removal of Pb(II) and Cu(II) from wastewater using activated carbon from cassava peels, J. Mater. Cycles Waste Manage., 16 (2014) 347–358.
[68] E. Pehlivan, T. Altun, Ş. Parlayici, Modified barley straw as a potential biosorbent for removal of copper ions from aqueous solution, Food Chem., 135 (2012) 2229–2234.
[69] T. Longlong, L. Dan, H. Lingxin, C. Shiwei, Q. Wei, L. Jing, W. Qiang, L. Zhan, W. Wang-suo, One-pot hydrothermal synthesis of carbonaceous nanocomposites for efficient decontamination of copper, RSC Adv., 5 (2015) 98041–98049.
[70] A.Z.M. Badruddoza, A.S.H. Tay, P.Y. Tan, K. Hidajat, M.S. Uddin, Carboxymethyl-β-cyclodextrin conjugated magnetic nanoparticles as nano-adsorbents for removal of copper ions: synthesis and adsorption studies, J. Hazard. Mater., 185 (2011) 1177–1186.
[71] X. Ren, J. Li, X. Tan, X. Wang, Comparative study of graphene oxide, activated carbon and carbon nanotubes as adsorbents for copper decontamination, Dalton Trans., 42 (2013) 5266–5274.
[72] G. Huang, W. Wang, X. Mi, W. Xie, Y. Liu, J. Gao, Preparation of graphene oxide aerogel and its adsorption for $Cu^{2+}$ ions, Carbon, 50 (2012) 4856–4864.
[73] R. Demir-Cakan, N. Baccile, M. Antonietti, M.M. Titirici, Carboxylate-rich carbonaceous materials via one-step hydrothermal carbonization of glucose in the presence of acrylic acid, Chem. Mater., 21 (2009) 484–490.
[74] C.-Y. Kuo, Water purification of removal aqueous copper (II) by as-grown and modified multi-walled carbon nanotubes, Desalination, 249 (2009) 781–785.
[75] U. Maheshwari, B. Mathesan, S. Gupta, Efficient adsorbent for simultaneous removal of Cu(II), Zn(II) and Cr(VI): kinetic, thermodynamics and mass transfer mechanism, Process Saf. Environ. Prot., 98 (2015) 198–210.
[76] N. Fiol, I. Villaescusa, M. Martínez, N. Miralles, J. Poch, J. Serarols, Sorption of Pb(II), Ni(II), Cu(II) and Cd(II) from aqueous solution by olive stone waste, Sep. Purif. Technol., 50 (2006) 132–140.
[77] N. Feng, X. Guo, S. Liang, Adsorption study of copper(II) by chemically modified orange peel, J. Hazard. Mater., 164 (2009) 1286–1292.
[78] J.C.P. Vaghetti, E.C. Lima, B. Royer, B.M. da Cunha, N.F. Cardoso, J.L. Brasil, S.L.P. Dias, Pecan nutshell as biosorbent to remove Cu(II), Mn(II) and Pb(II) from aqueous solutions, J. Hazard. Mater., 162 (2009) 270–280.
[79] P. Tasaso, Adsorption of copper using pomelo peel and depectinated pomelo peel, J. Clean Energy Technol., 2 (2014) 154–157.
[80] T. Aman, A.A. Kazi, M.U. Sabri, Q. Bano, Potato peels as solid waste for the removal of heavy metal copper(II) from waste water/industrial effluent, Colloids Surf., B, 63 (2008) 116–121.
[81] M. Kaur, P. Sharma, S. Kumari, Equilibrium studies for copper removal from aqueous solution using nanoadsorbent synthesized from rice husk, SN Appl. Sci., 1 (2019) 988, doi: 10.1007/s42452-019-1024-0.
[82] H. Aydın, Y. Bulut, Ç. Yerlikaya, Removal of copper(II) from aqueous solution by adsorption onto low-cost adsorbents, J. Environ. Manage., 87 (2008) 37–45.
[83] A. Witek-Krowiak, Analysis of temperature-dependent biosorption of $Cu^{2+}$ ions on sunflower hulls: kinetics, equilibrium and mechanism of the process, Chem. Eng. J., 192 (2012) 13–20.
[84] C.C. Ferrari, C.P. Ribeiro, A.M. Liserre, I. Moreno, S.P.M. Germer, J.M. de Aguirre, Spray Drying of Blackberry Juice using Maltodextrin or Gum Arabic as Carrier Agents, 6th International CIGR Technical Symposium – Towards a Sustainable Food Chain: Food Process, Bioprocessing and Food Quality Management, Nantes, France, April 18–20, 2011.
[85] K.Y. Lou, A.U. Rajapaksha, Y.S. Ok, S.X. Chang, Sorption of copper(II) from synthetic oil sands process-affected water (OSPW) by pine sawdust biochars: effects of pyrolysis temperature and steam activation, J. Soils Sediments, 16 (2016) 2081–2089.
[86] S. Zhao, N. Ta, X. Wang, Absorption of Cu(II) and Zn(II) from aqueous solutions onto biochars derived from apple tree branches, *Energies, 13* (2020) 3498, doi: 10.3390/en13133498.
[87] A.H. Sulaymon, A.A. Mohammed, T.J. Al-Musawi, Removal of lead, cadmium, copper, and arsenic ions using biosorption: equilibrium and kinetic studies, Desal. Water Treat., 51 (2013) 4424–4434.
[88] J.H. Park, Y.S. Ok, S.H. Kim, J.S. Cho, J.S. Heo, R.D. Delaune, D.C. Seo, Competitive adsorption of heavy metals onto sesame straw biochar in aqueous solutions, Chemosphere, 142 (2016) 77–83.
[89] A.G. Caporale, M. Pigna, A. Sommella, P. Conte, Effect of pruning-derived biochar on heavy metals removal and water dynamics, Biol. Fertil. Soils, 50 (2014) 1211–1222.
[90] A. Bogusz, P. Oleszczuk, R. Dobrowolski, Application of laboratory prepared and commercially available biochars to adsorption of cadmium, copper and zinc ions from water, Bioresour. Technol., 196 (2015) 540–549.

## Supporting information

### S1. Methods of blackberry residues characterization

In the experiments, blackberry biomass particles with a diameter less than 0.212 mm were used. In the beginning, the chemical and physical properties of the tested material were analyzed using several methods, descriptions of which are presented below.

- The experiments were performed on the extract from blackberry waste. The extracts were prepared by addition of 10 mL ethanol into 5 g of dried waste and incubated at 25°C for 24 h. The total phenolic content (TPC) was determined using the Folin–Ciocalteu's phenol reagent and the results were expressed as gallic acid equivalents. The TPC method was used to evaluate the ability of mate infusions to inhibit lipid oxidation by measuring the peroxide level during the initial stage of lipid oxidation. The TPC method response time is related to the period necessary for the absorbance (at 760 nm) to reach a maximum value. The low absorbance value of the reaction media after the addition of TPC reagents indicates the efficacy of the synthetic antioxidant of the test samples to inhibit lipid oxidation.

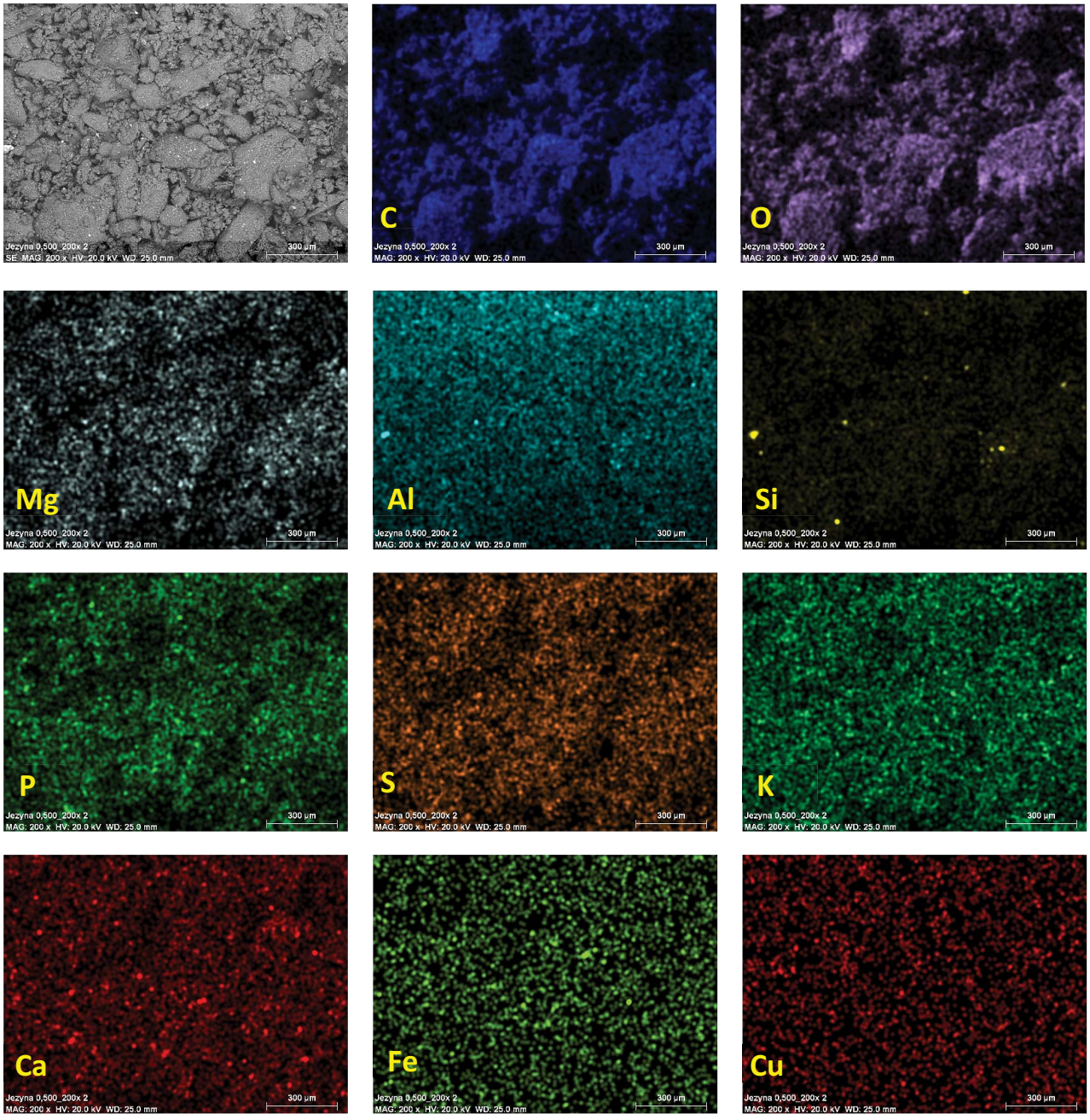


Fig. S1. SEM-EDX images (mapping) of the distribution and relative proportion (intensity) of defined elements (C, O, Mg, Al, Si, P, S, K, Ca, Fe, Cu) over the scanned area of blackberry residues (magn.: x200; scale bar: 300 µm).

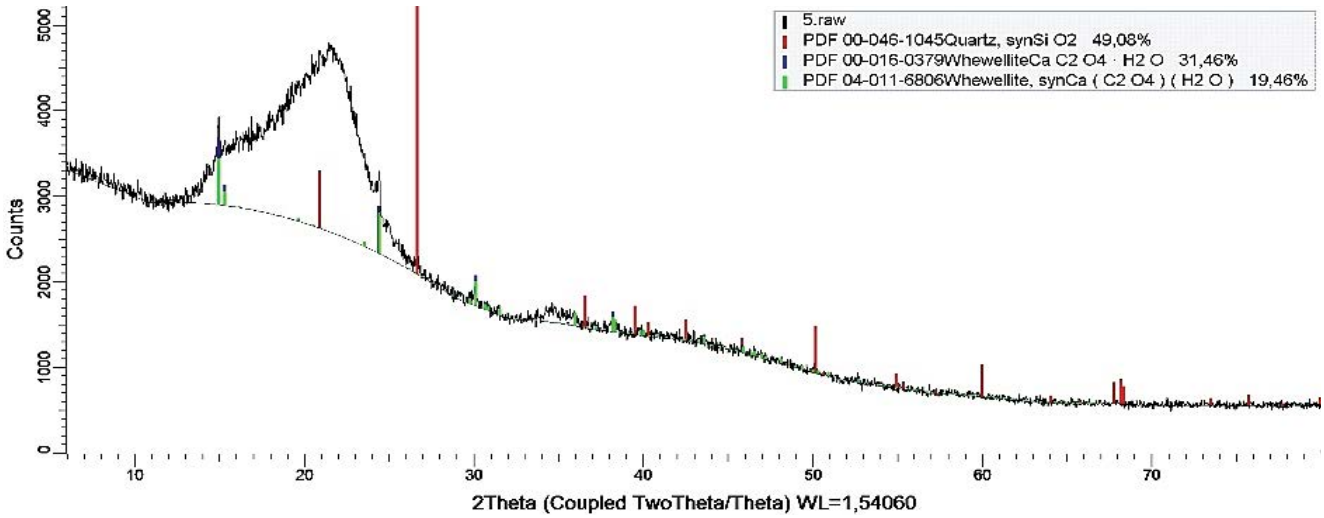


Fig. S2. X-ray diffraction pattern of blackberry residues.

Table S1
FTIR peaks of blackberry residues and their description

| FTIR wavelengths ($cm^{-1}$) | Band vibration characteristics |
|---|---|
| 3,286; 3,286.9 | Stretching O–H (water or other hydroxylated molecules, for example, alcohols) |
| 2,923.3; 2,923.8 | Asymmetric stretching C–H, $–CH_2–$ and $–CH_3$ (carboxylic acids) |
| 2,853.4; 2,854 | Stretching $–CH_3$, C–H |
| 1,742.4; 1,741.8 | Stretching C=O (e.g., esters) |
| 1,633.6; 1,641.8 | Stretching C–O bonds |
| 1,514.5; 1,515.1 | Stretching C=C, bending N–H bonds (aromatic ring) |
| 1,448.5; 1,452.2; 1,315.2; 1,316.3 | Deformation vibration C–H bonds |
| 1,225.9; 1,228.3 | Stretching C–O–C bonds |
| 1,027.9; 1,033 | Bending C–O bonds (polysaccharides) |

- Determination of total antioxidant capacity was performed by the ferric reducing ability of plasma (FRAP) assay. A 3 mL sample of FRAP solution (0.3 mol acetate buffer (pH 3.6), consisting of 10 mmol 2,4,6-tripyridyl-S-triazine (TPTZ) and 40 mmol $FeCl_3 \cdot 6H_2O$) and 100 μL of blackberry extract was kept at 38°C for 5 min and the absorbance was measured at 593 nm. The ferric-tripyridyl triazine ($Fe^{3+}$-TPTZ) complex is reduced to the ferrous ($Fe^{2+}$) form and as a result, an intense blue color appears. A standard solution of 1 mmol L-ascorbic acid was prepared using distilled water. The absorbance change was converted into a FRAP value, by relating the change of absorbance at 593 nm of the test sample to that of the standard solution of L-ascorbic acid (AA) and results were obtained as μmol AA/g.
- Methanol, ethanol, hydrochloric acid, sodium hypochlorite and acetone were used for high-performance liquid chromatography (HPLC) analysis (Sigma-Aldrich, Germany). The mobile phase used for the method included ultrapure Milli-Q water, methanol and acetic acid (Sigma-Aldrich, Germany). The HPLC standards for the analysis were purchased from Sigma-Aldrich. Stock standard solutions were prepared using dimethyl sulfoxide and/or methanol. Samples of dried blackberry material were extracted with a mixture of methanol/water/acetic acid. The homogenized sample was filtered using a paper filter. Next, the filtrate was evaporated at 90°C. The final volume of 10 mL was diluted with Milli-Q water. Chromatography analysis was carried out using HPLC apparatus. Compounds were detected at a wavelength of 280 nm.
- The elemental composition and mapping using a scanning electron microscopy (SEM) Hitachi S-3700N with an attached NORAN SIX energy-dispersive X-ray spectrometer (EDX) microanalyzer (UltraDry silicon drift type with resolution (FWHM) 129 eV, accelerating voltage: 20.0 kV).
- X-ray diffraction measurements were made using Bruker AXS D8 ADVANCE (Germany). In the configuration, the diffractometer is equipped with a Johansson monochromator (λCu $K_{\alpha 1}$ = 1.5406 Å) and silicon strip detector LynxEye. The minimum measurement angle is 0,6° 2Θ deg. The XRD powder diffraction method

Table S2
Various properties and composition of raw blackberry in a 100 g sample according to the literature

| Blackberry ingredients or properties | Content in a 100 g sample of raw blackberry | Blackberry ingredients or properties | Content in a 100 g sample of raw blackberry | Blackberry ingredients or properties | Content in a 100 g sample of raw blackberry (g) |
|---|---|---|---|---|---|
| Soluble solids | 6.9%–16.8% [S1–S6] | Flavonoids | 6–300 mg [S3,S12,S18,S19] | Arachidic acid C20:0 | <0.7% w/w [S23–S25] |
| Titratable acidity | [S1–S4,S6,S7] | Phenolic acids | 7–64 mg [S18,S20] | Total saturated acids | 6.5%–9% w/w [S23–S25] |
| pH | 2.6–3.9 [S1–S4,S7] | Lignans | 0.6 mg [S18,S21] | Total monosaturated acids | 14%–20% w/w [S23–S25] |
| Simple sugars | 2.6–13.9 g [S1,S7,S8] | Resveratrol | 1.8 μg [S22] | Total polyunsaturated acids | 58%–79% w/w [S23–S25] |
| Organic acids | 0.5–2.9 g [S1,S5,S8] | Trans-piceid | 3 μg [S18] | Ratio omega-6/omega-3 | 2.7%–3.5% [S23–S25] |
| Vitamin C | 1.2–11.9 mg [S4,S7] | Cis-piceid | 1.5 μg [S18] | Carotenoids (Lutein and β-carotene) in seeds | ~30 mg [S26] |
| Anthocyanins | 28–366 mg [S2,S6,S7,S9–S13] | Lauric acid C12:0 | <0.05% w/w [S23–S25] | Tocopherols (α-tocopherols, (β + γ) and δ-tocopherol) | 130–230 mg [S29,S30] |
| Phenolic monomers | 0.7–555 mg [S7,S12–S15] | Myristic acid C14:0 | <0.05% w/w [S23–S25] | β-Sitosterol | 85%, ~340 mg [S29] |
| Ellagic acid conjugates | 17–27 mg [S16] | Palmitic acid C16:0 | 2.2%–4.6% w/w [S23–S25] | Δ5-Avenasterol | 7%, ~28 mg [S23] |
| Phenolic polymers | 85–390 mg [S5,S13,S15,S16] | Stearic acid C18:0 | 2.1%–4.7% w/w [S23–S25] | Campesterol | 5%, ~20 mg [S23] |
| Carotenoids | 0.44–0.59 mg [S17] | Oleic acid C18:1 | 14%–20% w/w [S23–S25] | Δ7-Avenasterol and stigmasterol | 3%, ~12 mg [S23] |
| Ellagitannins | 84–130 mg (temperate climates) [S3,S14,S18] | Linoleic acid C18:2 | 42%–64% w/w [S23–S25] | Arachidic acid C20:0 | <0.7% w/w [S23–S25] |
| Ellagitannins | 200–500 mg (tropical highlands) [S3,S14,S18] | α-Linolenic acid C18:3 | 14%–18% w/w [S23–S25] | Total saturated acids | 6.5%–9% w/w [S23–S25] |
| Anthocyanins | 28–366 mg [S3,S12,S18,S19] | Flavonoids | 6–300 mg [S3,S12,S18,S19] | Total monosaturated acids | 14%–20% w/w [S23–S25] |

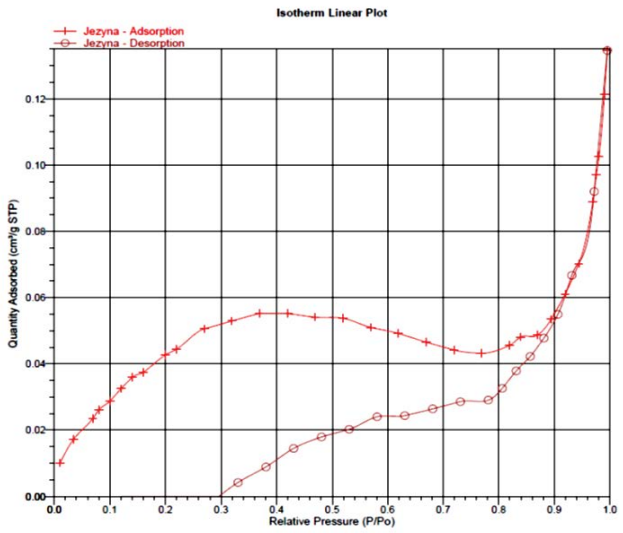


Fig. S3. The low-temperature BET adsorption and desorption isotherm linear plot (blackberry residues).

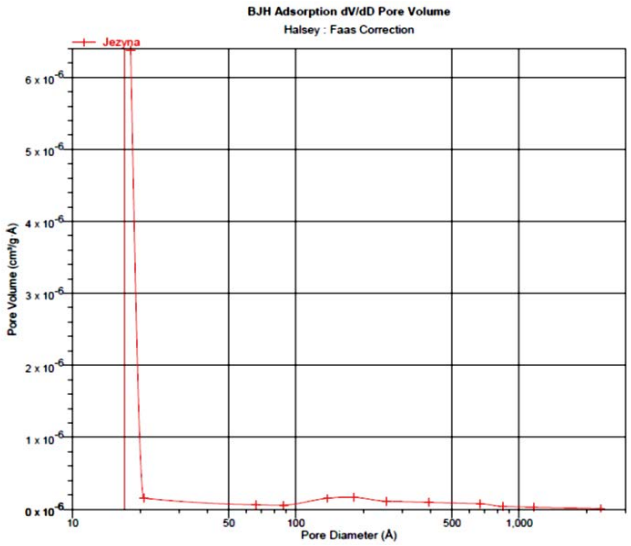


Fig. S5. Pore volume distribution (The Barrett–Joyner–Halenda Method) for adsorption *dV*/*dD* (blackberry residues).

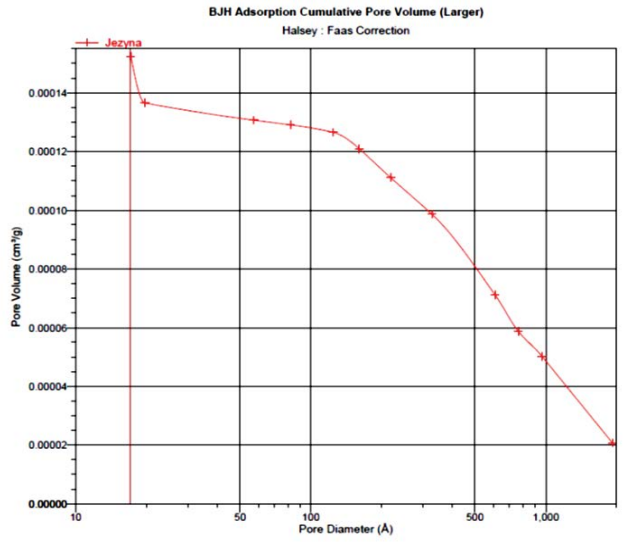


Fig. S4. Pore volume distribution (The Barrett–Joyner–Halenda Method) for adsorption (blackberry residues).

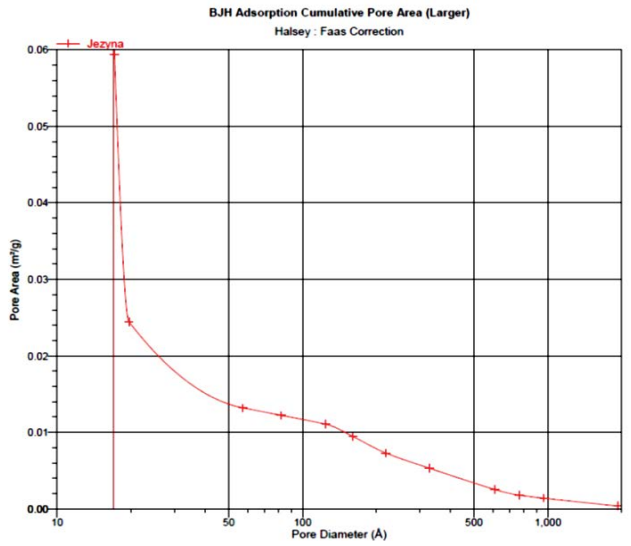


Fig. S6. Adsorption cumulative pore area (The Barrett–Joyner–Halenda Method).

needs the delivered sample to be carefully powdered. A standard measuring dish has a container for powder with a diameter of ca. 25 mm and ca. 1.5 mm depth. Before measurement, sample powder needs to be mildly pressed.

- The specific surface area and the average pore diameter by the Brunauer–Emmett–Teller (BET) method using Autosorb-iQ Station 2 (Quantachrome Instruments, USA).
- The pore volume was determined by Barrett–Joyner–Halenda method using Autosorb-iQ Station 2 (Quantachrome Instruments, USA).
- Thermogravimetry analyzed by Setup DTG, DTA 1200 (Setaram Solutions; temperature range 30°C–600°C; the rate of temperature increase 10°C/min; gas flow rate of nitrogen 20 mL/min).
- Investigation of electrokinetic zeta potential was carried out using Zetasizer Nano ZS (Malvern Instruments Ltd., United Kingdom) equipped with Autotitrator (MPT-2 Autotitrator). The apparatus uses a combination of electrophoresis and laser particle movement measurement based on the Doppler Effect. The instrument measures the rate of particle movement in the liquid after switching on the electric field. The speed of motion

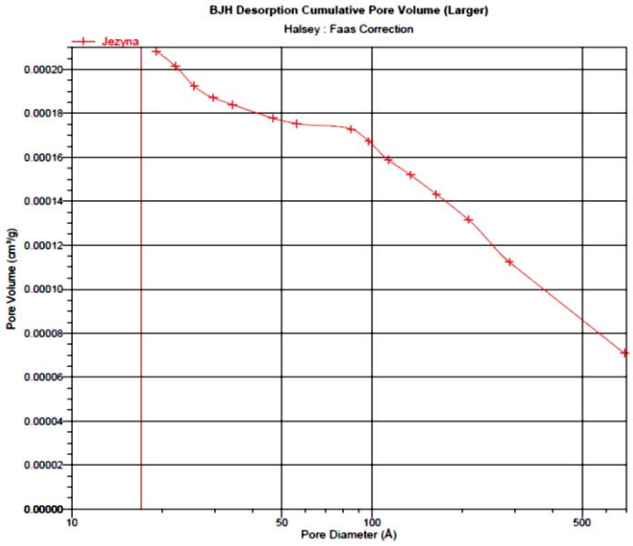


Fig. S7. Desorption cumulative pore volume (The Barrett–Joyner–Halenda Method).

of the particle is defined as its electrophoretic mobility, which is automatically calculated and converted to the zeta potential using Smoluchowski's Eq. (1).

$$\zeta = \frac{4\pi\eta}{\varepsilon} U \tag{S1}$$

where: $\zeta$ is zeta potential; $\pi$ is the constant; $\eta$ is the viscosity of the suspending liquid; $\varepsilon$ is the dielectric constant and $U$ is the electrophoretic mobility. Ash samples were dispersed in distilled water and the pH of the slurry was adjusted by the addition of 0.2 M HCl and 0.2 M KOH before measurements at room temperature (23°C ± 1°C) of electrophoretic mobility of particles.

- The morphology by SEM EVO-40 (Carl Zeiss, Germany).
- The surface structure analysis by a Fourier transform attenuated total reflection (FTIR-ATR) Spectrum 100 (Perkin-Elmer, Waltham, USA).

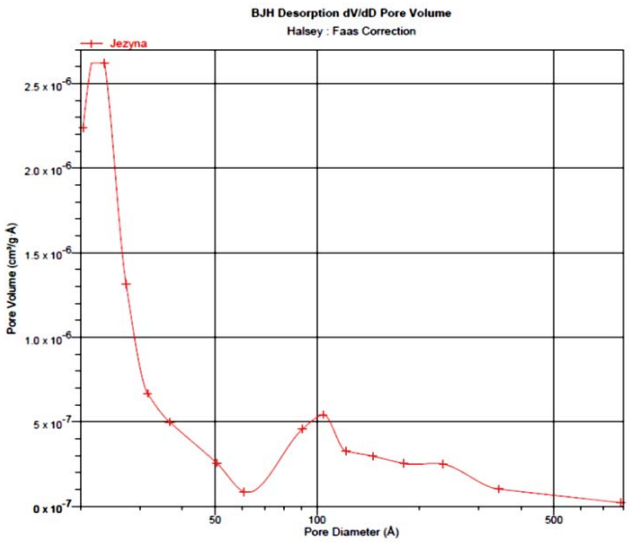


Fig. S8. Desorption pore volume *dV*/*dD* (The Barrett–Joyner–Halenda Method).

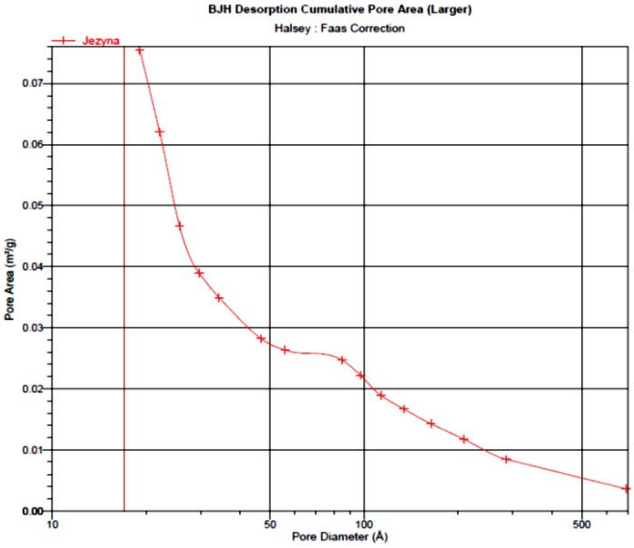


Fig. S9. Desorption cumulative pore area (The Barrett–Joyner–Halenda Method).

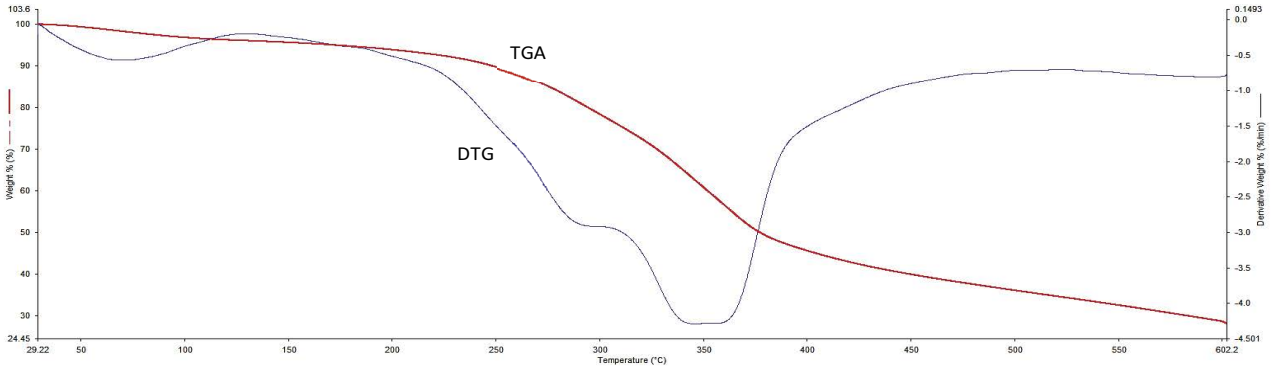


Fig. S10. Thermogravimetric curves of blackberry residues.

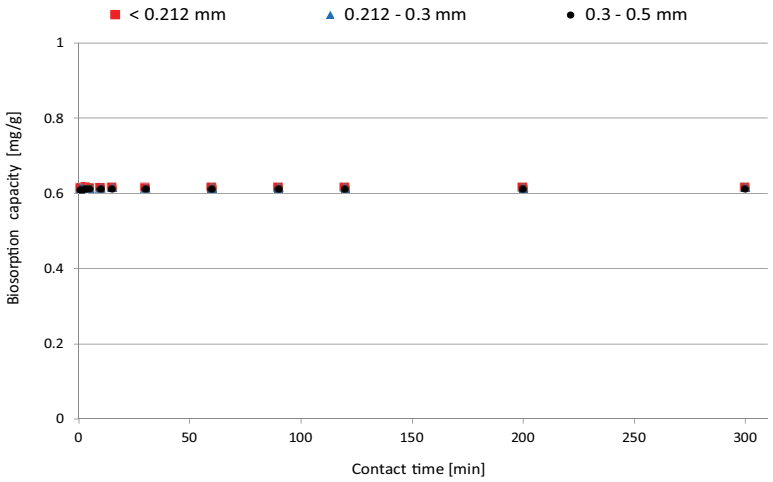


Fig. S11. The impact of contact time on the Cu(II) biosorption capacity (mg/g) depending on the blackberry particle size.

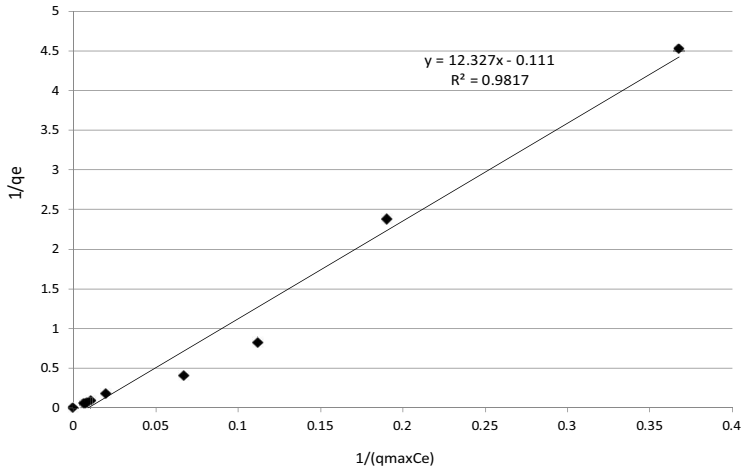


Fig. S12. Langmuir kinetic isotherm for the biosorption of Cu(II) with blackberry residues (particle size range 0.212–0.3 mm; biosorbent dosage 1 g/L; pH 4; initial concentration of Cu(II) 10 mg/L).

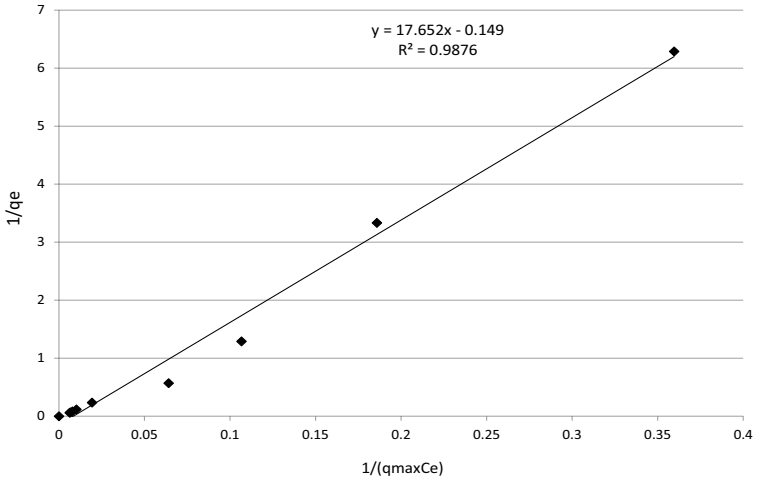


Fig. S13. Langmuir kinetic isotherm for the biosorption of Cu(II) with blackberry residues (particle size range 0.212–0.3 mm; biosorbent dosage 5 g/L; pH 4; initial concentration of Cu(II) 10 mg/L).

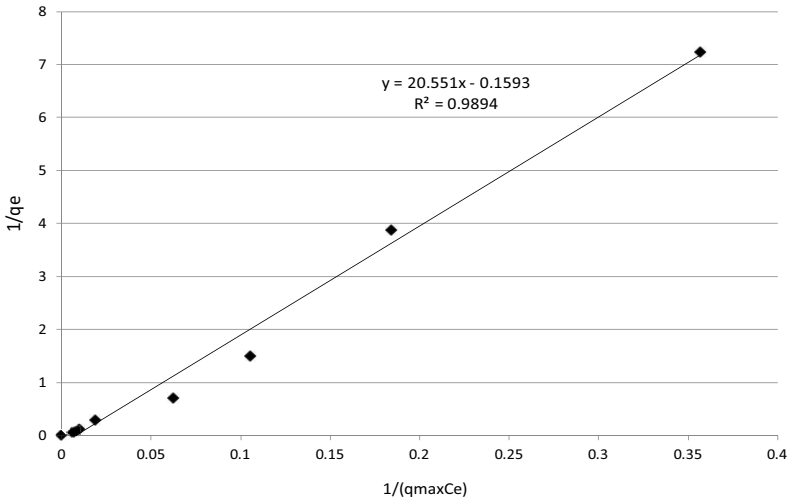


Fig. S14. Langmuir kinetic isotherm for the biosorption of Cu(II) with blackberry residues (particle size range 0.212–0.3 mm; biosorbent dosage 10 g/L; pH 4; initial concentration of Cu(II) 10 mg/L).

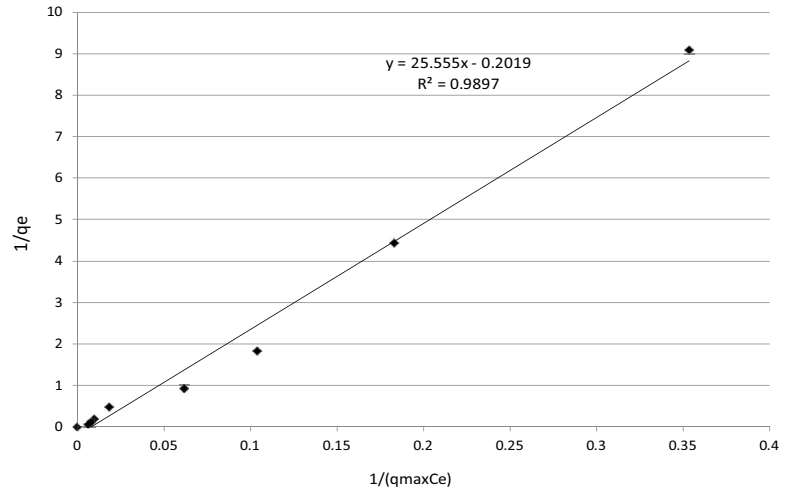


Fig. S15. Langmuir kinetic isotherm for the biosorption of Cu(II) with blackberry residues (particle size range 0.212–0.3 mm; biosorbent dosage 20 g/L; pH 4; initial concentration of Cu(II) 10 mg/L).

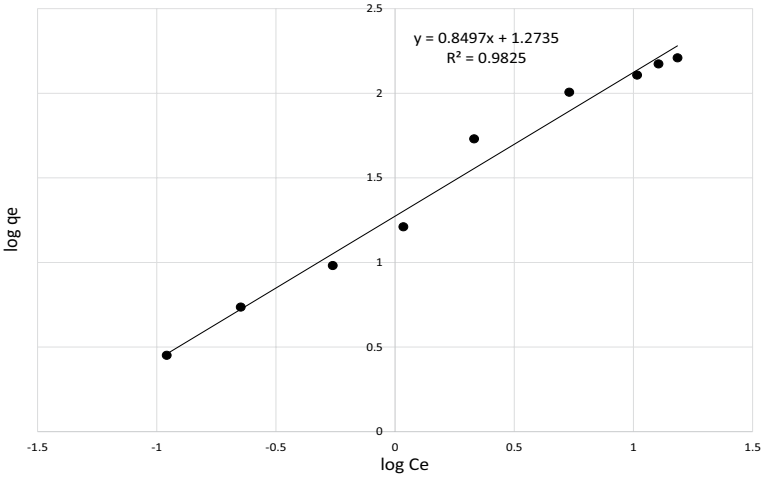


Fig. S16. Freundlich kinetic isotherm for the biosorption of Cu(II) with blackberry residues (particle size range 0.212–0.3 mm; biosorbent dosage 1 g/L; pH 4; initial concentration of Cu(II) 10 mg/L).

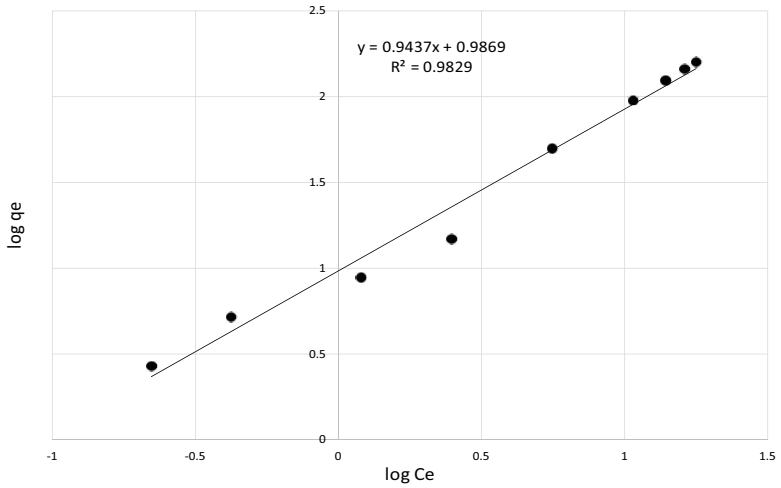


Fig. S17. Freundlich kinetic isotherm for the biosorption of Cu(II) with blackberry residues (particle size range 0.212–0.3 mm; biosorbent dosage 5 g/L; pH 4; initial concentration of Cu(II) 10 mg/L).

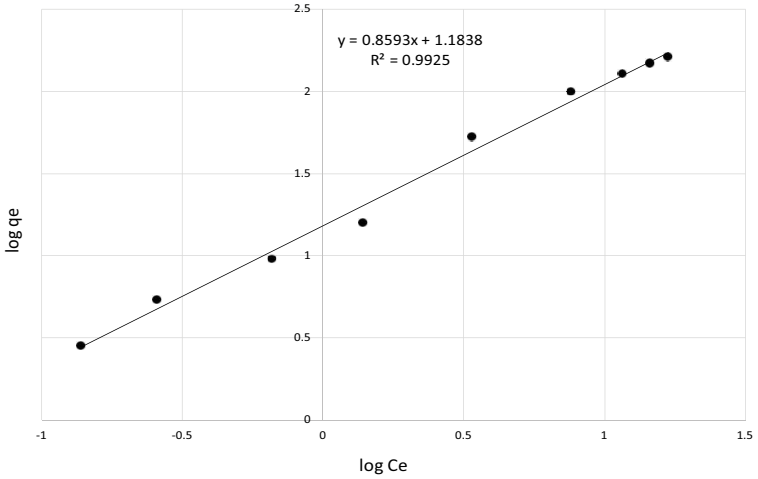


Fig. S18. Freundlich kinetic isotherm for the biosorption of Cu(II) with blackberry residues (particle size range 0.212–0.3 mm; biosorbent dosage 10 g/L; pH 4; initial concentration of Cu(II) 10 mg/L).

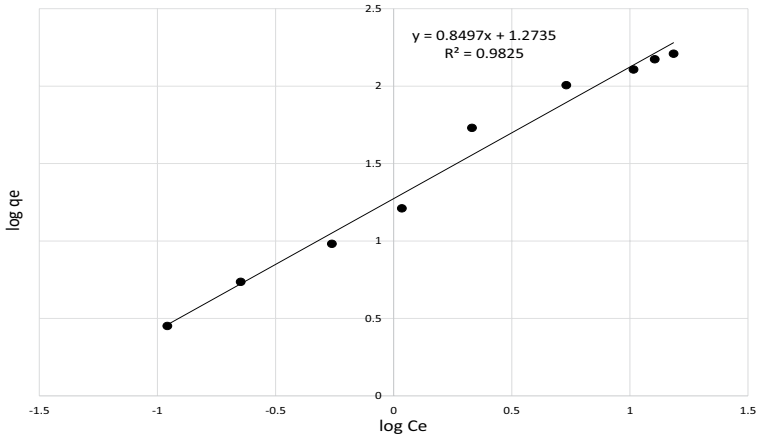


Fig. S19. Freundlich kinetic isotherm for the biosorption of Cu(II) with blackberry residues (particle size range 0.212–0.3 mm; biosorbent dosage 20 g/L; pH 4; initial concentration of Cu(II) 10 mg/L).

## References


[S1] H.-J. Fan-Chiang, R.E. Wrolstad, Sugar and nonvolatile acid composition of blackberries, J. AOAC Int., 93 (2010) 956–965.

[S2] C.E. Finn, B.C. Strik, B.M. Yorgey, M.E. Peterson, J. Lee, R.R. Martin, H.K. Hall, 'Columbia Star' thornless trailing blackberry, HortScience, 49 (2014) 1108–1112.

[S3] C. Mertz, V. Cheynier, Z. Günata, P. Brat, Analysis of phenolic compounds in two blackberry species (*Rubus glaucus* and *Rubus adenotrichus*) by high-performance liquid chromatography with diode array detection and electrospray ion trap mass spectrometry, J. Agric. Food Chem., 55 (2007) 8616–8624.

[S4] R.H. Thomas, F.M. Woods, W.A. Dozier, R.C. Ebel, M. Nesbitt, B. Wilkins, D.G. Himelrick, Cultivar variation in physicochemical and antioxidant activity of Alabama-grown blackberries, Small Fruits Rev., 4 (2005) 57–71.

[S5] U. Vrhovsek, L. Giongo, F. Mattivi, R. Viola, A survey of ellagitannin content in raspberry and blackberry cultivars grown in Trentino (Italy), Eur. Food Res. Technol., 226 (2008) 817–824.

[S6] S.Y. Wang, L. Bowman, M. Ding, Methyl jasmonate enhances antioxidant activity and flavonoid content in blackberries (*Rubus* sp.) and promotes antiproliferation of human cancer cells, Food Chem., 107 (2008) 1261–1269.

[S7] R. Veberic, F. Stampar, V. Schmitzer, V. Cunja, A. Zupan, D. Koron, M. Mikulic-Petkovsek, Changes in the contents of anthocyanins and other compounds in blackberry fruits due to freezing and long-term frozen storage, J. Agric. Food Chem., 62 (2014) 6926–6935.

[S8] M. Mikulic-Petkovsek, V. Schmitzer, A. Slatnar, F. Stampar, R. Veberic, Composition of sugars, organic acids, and total phenolics in 25 wild or cultivated berry species, J. Food Sci., 77 (2012) C1064–C1070.

[S9] A.M. Conner, C.E. Finn, T.K. McGhie, P.A. Alspach, Genetic and environmental variation in anthocyanins and their relationship to antioxidant activity in blackberry and hybridberry cultivars, J. Am. Soc. Hortic. Sci., 130 (2005) 680–687.

[S10] H. Fan-Chiang, R.E. Wrolstad, Anthocyanin pigment composition of blackberries, J. Food Sci., 70 (2005) C198–C202.

[S11] J. Scalzo, A. Currie, J. Stephens, T. McGhie, P. Alspach, The anthocyanin composition of different *Vaccinium*, *Ribes* and *Rubus* genotypes, Biofactors, 34 (2008) 13–21.

[S12] S. Sellappan, C.C. Akoh, G. Krewer, Phenolic compounds and antioxidant capacity of Georgia-grown blueberries and blackberries, J. Agric. Food Chem., 50 (2002) 2432–2438.

[S13] C. Vasco, K. Riihinen, J. Ruales, A. Kemal-Eldin, Phenolic compounds in Rosaceae fruits from Ecuador, J. Agric. Food Chem., 57 (2009) 1204–1212.

[S14] A. Acosta-Montoya, F. Vaillant, S. Cozzano, C. Mertz, A.M. Perez, M.V. Castro, Phenolic content and antioxidant capacity of tropical highland blackberry (*Rubus adenotrichus* Schltdl.) during three edible maturity stages, Food Chem., 119 (2010) 1497–1501.

[S15] A. Gancel, A. Feneuil, O. Acosta, A.M. Perez, F. Vaillant, Impact of industrial processing and storage on major polyphenols and the antioxidant capacity of tropical highland blackberry (*Rubus adenotrichus*), Food Res. Int., 44 (2011) 2243–2251.

[S16] M. Gasperotti, D. Masuero, U. Vrhovsek, G. Guella, F. Mattivi, Profiling and accurate quantification of *Rubus ellagitannins* and ellagic acid conjugates using direct UPLC-Q-TOF HDMS and HPLC-DAD analysis, J. Agric. Food Chem., 58 (2010) 4602–4616.

[S17] D. Marinova, F. Ribarova, HPLC determination of carotenoids in Bulgarian berries, J. Food Compos. Anal., 20 (2007) 370–374.

[S18] F. Vaillant, Chapter 25 – Blackberries, In: Nutritional Composition and Antioxidant Properties of Fruits and Vegetables, 2020, pp. 407–422, doi: 10.1016/B978-0-12-812780-3.00025-8.

[S19] M. Zia-Ul-Haq, M. Riaz, V. De Feo, H.Z.E. Jaafar, M. Moga, *Rubus fruticosus* L.: constituents, biological activities and health related uses, Molecules, 19 (2014) 10998–11029.

[S20] L. Kaume, L.R. Howard, L. Devareddy, The blackberry fruit: a review on its composition and chemistry, metabolism and bioavailability, and health benefits, J. Agric. Food Chem., 60 (2012) 5716–5727.

[S21] W.M. Mazur, M. Uehara, K. Wähälä, H. Adlercreutz, Phyto-oestrogen content of berries, and plasma concentrations and urinary excretion of enterolactone after a single strawberry-meal in human subjects, Br. J. Nutr., 83 (2000) 381–387.

[S22] X. Huang, G. Mazza, Simultaneous analysis of serotonin, melatonin, piceid and resveratrol in fruits using liquid chromatography tandem mass spectrometry, J. Chromatogr. A, 1218 (2011) 3890–3899.

[S23] V. Van Hoed, N. De Clercq, C. Echim, M. Andjelkovic, E. Leber, K. Dewettinck, R. Verhé, Berry seeds: a source of specialty oils with high content of bioactives and nutritional value, J. Food Lipids, 16 (2009) 33–49.

[S24] O. Radočaj, V. Vujasinović, E. Dimić, Z. Basić, Blackberry (*Rubus fruticosus* L.) and raspberry (*Rubus idaeus* L.) seed oils extracted from dried press pomace after longterm frozen storage of berries can be used as functional food ingredients, Eur. J. Lipid Sci. Technol., 116 (2014) 1015–1024.

[S25] A. Wajs-Bonikowska, A. Stobiecka, R. Bonikowski, A. Krajewska, M. Sikora, J. Kula, A comparative study on composition and antioxidant activities of supercritical carbon dioxide, hexane and ethanol extracts from blackberry (*Rubus fruticosus*) growing in Poland, J. Sci. Food Agric., 97 (2017) 3576–3583.

[S26] V.R. de Souza, P.A.P. Pereira, T.L.T. da Silva, L.C. de Oliveira Lima, R. Pio, F. Queiroz, Determination of the bioactive compounds, antioxidant activity and chemical composition of Brazilian blackberry, red raspberry, strawberry, blueberry and sweet cherry fruits, Food Chem., 156 (2014) 362–368.